Journal of Power Sources 195 (2010) 685–702

Contents lists available at ScienceDirect

Journal of Power Sources

journal homepage: www.elsevier.com/locate/jpowsour

Review

A review of integration strategies for solid oxide fuel cells

Xiongwen Zhang[a,b], S.H. Chan[b], Guojun Li[a,*], H.K. Ho[b], Jun Li[a], Zhenping Feng[a]

[a] School of Energy & Power Engineering, Xi'an Jiaotong University, Shaanxi 710049, China
[b] Fuel Cells Strategic Research Program, School of Mechanical and Aerospace Engineering, Nanyang Technology University, Singapore 639798, Singapore

ARTICLE INFO

Article history:
Received 19 June 2009
Received in revised form 25 July 2009
Accepted 29 July 2009
Available online 5 August 2009

Keywords:
Solid oxide fuel cell
Integration strategy
Hybrid system
Review

ABSTRACT

Due to increasing oil and gas demand, the depletion of fossil resources, serious global warming, efficient energy systems and new energy conversion processes are urgently needed. Fuel cells and hybrid systems have emerged as advanced thermodynamic systems with great promise in achieving high energy/power efficiency with reduced environmental loads. In particular, due to the synergistic effect of using integrated solid oxide fuel cell (SOFC) and classical thermodynamic cycle technologies, the efficiency of the integrated system can be significantly improved. This paper reviews different concepts/strategies for SOFC-based integration systems, which are timely transformational energy-related technologies available to overcome the threats posed by climate change and energy security.

Contents

Abbreviations: APU, auxiliary power unit; ASU, air separation unit; AR, absorption refrigeration; BoP, balance of plant; BWR, boiling water reactor; CHP, combined heat and power; COE, cost of electricity; CB, combustor; CP, compressor; GT, gas turbine; HE, heat exchanger; HHV, high heat value; HP, high pressure; HRSG, heat recovery steam generator; HRU, heat recovery unit; HSD, hydrogen separation device; HTGR, high temperature gas-cooled reactor; IP, intermediate pressure; JAERI, Japan Atomic Energy Research Institute; LHV, low heat value; LP, low pressure; MHR, modular helium reactor; PEM, proton exchange membrane; PV, photovoltaic; PWR, pressurized water reactor; SECA, solid-state energy conversion alliance; S–I, sulfur–iodine; SOFC, solid oxide fuel cell; TB, turbine; TPV, thermophotovoltaic; VS, vessel.

* Corresponding author. Tel.: +86 29 82668728; fax: +86 29 82665062.
E-mail addresses: xwenz@mailst.xjtu.edu.cn (X. Zhang), mshchan@ntu.edu.sg (S.H. Chan), liguojun@mail.xjtu.edu.cn (G. Li).

0378-7753/$ – see front matter © 2009 Elsevier B.V. All rights reserved.
doi:10.1016/j.jpowsour.2009.07.045

1. Introduction

Power generation and the related environmental impacts have become important issues across the world [1,2]. Today, electrical power is provided mainly by conventional power generation technologies that rely on fossil fuel combustion, which generates soot and sulfur compounds, in addition to other noxious emissions. The combustion of fossil fuels is widely understood to contribute to both global warming and local air pollution. Advanced clean energy systems must be developed urgently, allowing us to make the shift from a fossil fuel-based economy to a new paradigm in a progressive manner. In 1997, the US Department of Energy launched its Vision 21st program [3,4], which was essentially meant to conduct conceptual feasibility studies to assess high-efficiency fossil fuel power plants and thereby develop the core technologies for a fleet of fuel-flexible, multi-product energy plants with an electricity generation efficiency higher than 75% for gas and 60% for coal. The fuel cell is an emerging alternative to traditional power generation systems; it offers the potential for higher electrical efficiencies and lower emissions [5,6]. Various fuel cells are available today, differentiated by the electrolyte used and its operating temperature. The electrolyte of a solid oxide fuel cell (SOFC) consists of a solid, fully dense oxide metal (typically yttria (Y_2O_3) stabilized zirconia (ZrO_2) or YSZ). The anode of a SOFC is typically made of a nickel cermet, such as Ni-YSZ, while the cathode is made of strontium (Sr) doped with lanthanum manganite ($LaMnO_3$) [5]. The fact that all the components in a SOFC are solid structures makes it possible for the cells to be constructed in any geometry. The SOFC operates in the range of 600–1000 °C, which allows it to combine with other conventional thermal cycles to yield improved thermal efficiency. The hybrid SOFC system is considered to be a key technology in achieving the goals of Vision 21st [7] on account of the many advantages it offers over other systems.

First, there are no moving components in the fuel cell (except for balance of plant (BoP) components). Noise and vibrations associated with mechanical motion during operation are practically non-existent. This makes it possible to install the system in urban or suburban areas as a distributed power generation plant. Without moving parts, we would expect enhanced reliability and lower maintenance cost. Secondly, SOFCs (by virtue of high-temperature operation) can extract hydrogen from a variety of fuels. SOFC is the most sulfur-resistant (as H_2S and COS) fuel cell. It can tolerate sulfur-containing compounds at concentrations higher than other types of fuel cells [8]. In addition, it is not poisoned by carbon monoxide (CO); in fact, CO can be used as a fuel. These features allow SOFCs to be fed with gases derived from either solid or liquid fuels. This advantage is beneficial for coal-based central power generation and in vehicles that are powered by diesel or gasoline fuel [9–11]. Thirdly, the size of a SOFC module is flexible, thus allowing it to be constructed for use in any power range – from watts to megawatts. Therefore, a SOFC or its hybrid may be built for stationary applications (central power generation and distributed power generation) or as an auxiliary power unit (APU) for vehicles. The attributes of a SOFC and its hybrid system are summarized in Table 1 [9,12–19].

Integration strategies for SOFC hybrid systems are generally determined by the application requirements. In most cases, both efficiency and emissions are considered first in the design of these hybrid systems. However, in some cases (such as for aerospace and naval vessel applications), reliability and low noise levels may be more important. In the following sections, we present a thorough review of different integration concepts/strategies for SOFC-based hybrid systems.

2. SOFC fundamentals

SOFCs convert the chemical energy of a fuel directly into electrical energy through electrochemical reactions that are driven by the difference in the oxygen chemical potential between the anode and cathode of the cell. Oxygen ions migrate through the electrolyte to the anode where they are consumed by fuel oxidation. The electrochemical reaction in a SOFC is generally fuelled by hydrogen. At the cathode side:

$$(1/2)O_2 + 2e^- \rightarrow O^{2-}. \quad \text{(R1)}$$

At the anode side:

$$H_2 + O^{2-} \rightarrow H_2O + 2e^-. \quad \text{(R2)}$$

The SOFC consumes the hydrogen that is produced from natural gas through either internal or external steam reforming. The fuel reforming is endothermic reaction. The heat can be supplied by the overpotential loss and entropy change heat for internal reforming of high-temperature fuel cells including SOFC and MCFC. The chemical reactions include the methane reforming process and the water gas-shift reaction as follows:

$$\text{Steamreforming}: \quad CH_4 + H_2O \rightarrow CO + 3H_2 \quad \text{(R3)}$$

$$\text{Gas-shifting}: \quad CO + H_2O \rightarrow CO_2 + H_2. \quad \text{(R4)}$$

At the anode side, the carbon monoxide is electro-oxidized by oxygen ions, thus producing carbon dioxide and electrons:

$$CO + O^{2-} \rightarrow CO_2 + 2e^-. \quad \text{(R5)}$$

Although hydrogen is thought to be an ideal fuel for the future, there are issues associated with generation, storage, distribution, etc. In the required reforming processes, about 20–30% of the fuel energy is lost [20]. Studies have reported that it is possible for a SOFC to be directly fuelled with dry hydrocarbon [21,22]. The hydrocarbon is electro-oxidized at the anode as follows:

$$C_nH_{2n+2} + (3n+1)O^{2-} \rightarrow nCO_2 + (n+1)H_2O + (6n+2)e^- \quad \text{(R6)}$$

The stacks that operate directly on hydrocarbons need to be different from traditional stacks. The development of direct-fuel utilization SOFCs is still in its infancy; therefore, the direct hydrocarbon SOFC will not be considered in this review.

The reforming of hydrocarbons may take place either externally or internally in the SOFC system. Fig. 1 shows the electrochemical reactions in a SOFC stack that uses an internal steam reforming process. Part of the hydrocarbon fuel is reformed in an indirect internal reforming unit and the rest is directly reformed on the cells. Part of the heat that is released due to irreversible electrochemical reactions is utilized in the internal reforming process. The depleted fuel still contains some unutilized combustible fuel, such as hydrogen

Table 1
Potential attributes of a SOFC and related integration approaches [9,12–19].

Advantages	
Efficiency (achievable)	Stand-alone: 55%; hybrid: 60% (HHV) for coal-based, 75% (LHV) for gas-based, >55% for nuclear-based; CHP: thermal efficiency 85%
Environmental performance	Emissions: near zero of NO_x and SO_x; sequestration capable
Fuel flexibility	Hydrogen; liquefied natural gas; pipeline natural gas; diesel; coal synthesis gas; fuel oil; gasoline; biogases
Size flexibility	Range from watts to megawatts
Cogeneration capable	SOFC/TB based on Brayton cycle; SOFC/TB based on Rankine cycle; SOFC/HAT cycle; CHP; SOFC/TPV; SOFC/PEM; SOFC/AR
Disadvantages	
Poor thermal shock	Cracking risk due to the thermal stress
Long start-up	Several hours
High COE	US$800 per kW achievable [9]
Low acceptable fuel impurity	Sulfur removal and ash/residue disposal required, sulfur as H_2S and COS < 1 ppm
Carbon deposition	Hydrocarbon decomposition

and carbon monoxide. The unutilized fuel is routed to a combustor for oxidation. This combustor may be integrated into the SOFC stack or can be stand-alone.

3. Basic hybrid integration strategies

Availability, an important thermodynamic term, should be obeyed in plant hybrid systems. Specifically, one system (or cycle) needs to supply enough material or heat to meet the requirements of another system (or cycle). With regard to availability, the hybrid system could be built to operate via either thermal coupling or fuel coupling. Two thermal coupling schemes have been proposed for the exchange of thermal energy between the SOFC system and the objective combined cycle. In one scheme known as direct integration, the carrying medium of one cycle is directly sent to the other cycle via the working fluid. Under this integration scheme, both cycles operate with the same working fluid and at the same pressure. The other thermal coupling scheme, in which the thermal energy is utilized indirectly through a heat exchanger, is known as indirect integration, whereby the heat source cycle and the heat sink cycle operate with different working fluids and at different pressures. The fuel coupling scheme is used to configure the integration system of a SOFC either through the hydrogen production cycle or using a fuel reformer.

3.1. Direct thermal coupling scheme

Traditional thermodynamic power generation cycles are nothing more than Brayton or Rankine cycles or modifications thereof. The Rankine cycle is essentially a heat engine with a vapor power cycle. The commonly used working fluid is water, and the system operates in the liquid–vapor mode. Thus, the Rankine cycle cannot be combined with a SOFC using the direct thermal coupling scheme. Due to the use of a gas-based working fluid, the Brayton cycle is a favorable candidate for SOFC integration.

3.1.1. Pressurized SOFC + Brayton cycle

The combined SOFC and Brayton cycle is a typical direct thermal coupling scheme. Fig. 2 shows the configuration of a pressurized SOFC with a gas turbine (GT) engine. In this system, the compressed air is channeled to the cathode of a SOFC for oxygen reduction. Since

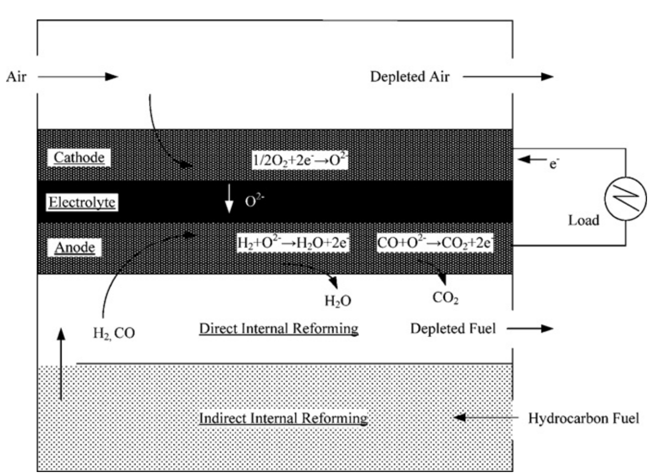

Fig. 1. The electrochemical reaction in a SOFC that features internal fuel reforming.

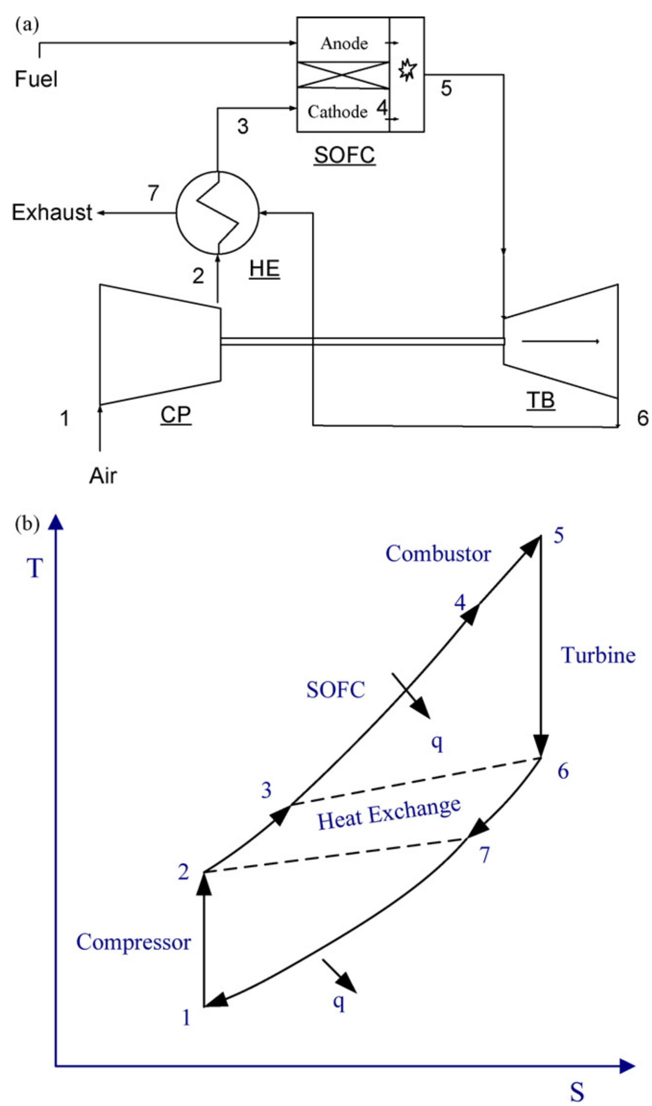

Fig. 2. Pressurized SOFC and gas turbine: (a) SOFC–GT system configuration and (b) *T–S* diagram for a Brayton cycle.

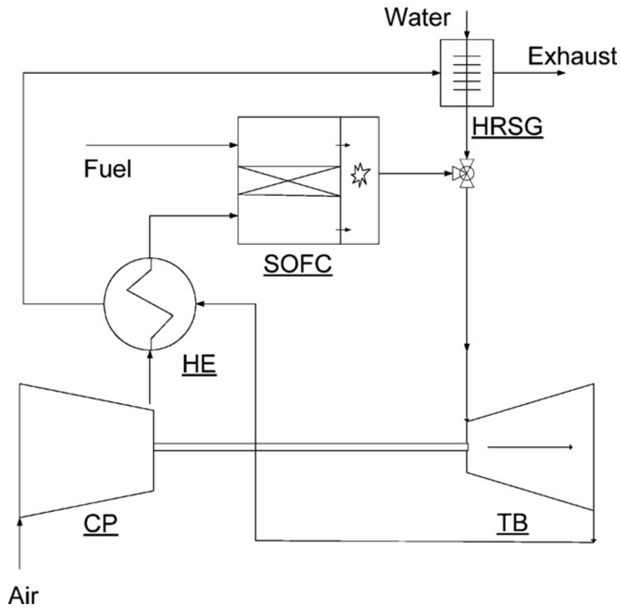

Fig. 3. A pressurized SOFC and gas turbine integrated with Cheng cycle.

the net chemical process in the SOFC is exothermic, both the air and fuel temperatures increase through the flow chambers of the SOFC. Fig. 2(b) shows the ideal temperature–entropy (*T*–*S*) diagram assuming no pressure loss for the Brayton cycle in association with the configuration in Fig. 2(a). The change between states 4 and 5 denotes the addition of heat from the combustor. The combustor is housed inside the SOFC following the approach developed by Siemens-Westinghouse [23–26]. The non-utilized fuel in the product gases is combusted in the combustor. This configuration serves as a basic building block for a SOFC–GT hybrid system. Most recent studies have focused on this scheme [26–47]. It is challenging to validate system efficiency due to the lack of experimental data for specific fuel cell systems and the balance of plants (BoPs); therefore, the system efficiencies reported by most simulation studies to date have focused on typical hybrid systems. With reference to the published data [26–47], the optimum efficiency for the combined pressurized SOFC–GT engine can reach 60% (LHV) for a natural gas-fed system with no additional fuel burned in the combustor. A demonstration of 200 kW SOFC–GT hybrid system launched by Mitsubishi Heavy Industries (MHI) showed that the electrical efficiency reached 52% (LHV) in the actual operations [47].

Based on this scheme, we can develop a more complicated hybrid thermodynamic system consistent with the designed conditions. The air compression process may be separated into two stages with an intercooler mounted between the two compressors [48] to decrease the air inlet temperature of the heat exchanger (HE), thus improving the utilization of exhaust heat. However, as noted by Williams et al. [48], the inlet air temperature of the SOFC will also decrease, which is undesirable for a SOFC. Therefore, the introduction of an intercooler is only recommended for high operating pressures, as shown in Refs. [49,50]. Zhang et al. [51] inserted an additional reheater between the HE and the SOFC by using part of the combustor exhaust gas as a heat source to maintain the minimum temperature of the SOFC stack. Araki et al. [52] added a low-temperature SOFC before a high-temperature SOFC in serial connection. The simulation results show that the efficiency of the combined cycle with two-stage SOFC is a little higher than that by high-temperature SOFC only [52]. Similar to the configuration of the two-stage SOFC integration system, a multi-stage SOFC combined cycle was proposed in the reference [53]. In this system, a few high fuel utilization SOFC stages were integrated with Brayton cycle for specially CO_2 capture. About 10% improvement of efficiency is possibility achieved for this kind of integration system comparing to that of the normal CO_2 recovery amine process [53].

3.1.2. Pressurized SOFC + Brayton cycle + Cheng cycle

Cheng cycle is an exhaust heat recovery cycle for specially optimizing the performance of Brayton cycle. Fig. 3 shows a configuration of Cheng cycle combined with SOFC and Brayton cycle. A heat recovery steam generator (HRSG) is added for producing the steam, which is injected into the gases before the turbine. The exhaust heat is utilized in HRSG, thus increasing the system energy efficiency. Because the turbine is a mass-flow device, combining the steam with the high-temperature gases will increase the total electrical power produced. Part of the steam produced in the HRSG can also be used for steam load. Therefore, Cheng cycle is a good option for following the electrical loads or steam loads via controlling the steam injection. Simulation results showed that the addition of a Cheng cycle to the pressurized SOFC/Brayton cycle improved the electrical efficiency by 1–3% [54]. But Cheng cycle decreases the temperature in the interior of the turbine, which permits to gain more efficiency via increasing the temperature of the fuel combustion [55].

3.1.3. Non-pressurized SOFC + Brayton cycle

Fig. 4 shows a non-pressurized SOFC combined with the Brayton cycle. Under this approach, the SOFC inlet air is taken from the gas turbine exhaust. The SOFC stack operates close to atmospheric pressure. Due to gas expansion through the turbine, the minimum inlet temperature of the SOFC may not be attained if the operating temperature of the fuel cell is too high or if the expansion ratio of the turbine is too large. Therefore, an intermediate-temperature SOFC is favored over this hybrid scheme. The maximum expansion ratio of the turbine is determined by the fuel cell operating temperature given a fixed turbine inlet temperature (TIT). The optimum efficiency of the SOFC in this hybrid scheme is expected to be 55% [48]. Additionally, the temperature of the exhaust gas is generally higher than that of the pressurized SOFC system, thus exhibiting less effective waste heat recovery. The optimum efficiency of this hybrid scheme is about 5% lower than that of the pressurized SOFC system with no additional fuel burned in the gas turbine combustor [48].

3.1.4. Pressurized SOFC + Brayton cycle + air reheating

The SOFC requires the inlet air temperature to be above a certain minimum temperature. However, if the operating temperature of a SOFC is too high or the expansion ratio of the turbine is too large, this requirement is difficult to meet solely through the recovery of turbine exhaust heat. As mentioned in Refs. [48,51], we can route part of the hot exhaust gas from the SOFC to reheat the air before it enters the SOFC by using a recuperator or by the exhaust gas recirculation (EGR) method. Fig. 5 presents a SOFC–GT hybrid system with a gas booster (GB) recirculating the exhaust of a SOFC to heat up the cathode inlet air. This method (see Fig. 5) achieves higher optimum pressure ratio, and its optimum efficiency is about 5% higher than that of the recuperative air preheating method [51]. Moreover, the natural gas is usually supplied as the fuel and is partially reformed in a pre-reformer (as in the case of the Siemens-Westinghouse design). As shown in Fig. 5, the heat requirement due to the endothermic reforming process is met by routing a percentage of the hot depleted fuel from the anode to the pre-reformer.

3.1.5. SOFC + PEM fuel cell

A hybrid system that comprises a SOFC combined with a polymer electrolyte membrane fuel cell (PEMFC) has been reported in the literatures [18,56,57]. In this system, the PEMFC makes use of the internal reforming ability of the SOFC to produce hydrogen,

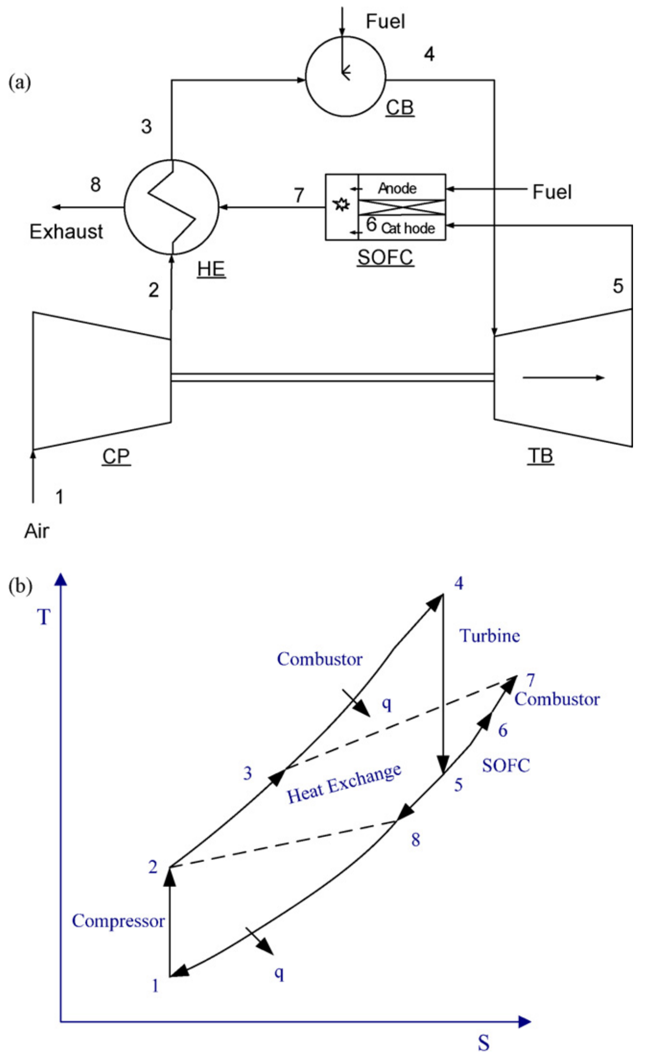

Fig. 4. Non-pressurized SOFC and gas turbine: (a) SOFC–GT system configuration and (b) *T*–*S* diagram for a Brayton cycle.

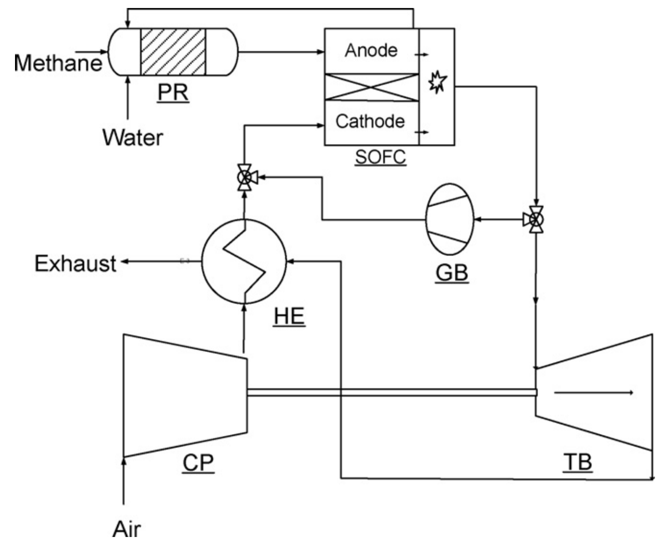

Fig. 5. A pressurized SOFC system with recirculated air reheating and gas turbine.

which is necessary for PEMFC operation. The heat released from electrochemical reactions in the SOFC is utilized by the internal reforming process. Fig. 6 shows the PEMFC schematic configuration. Natural gas enters the SOFC at the location where the fuel reforming and the electrochemical oxidation processes occur. The SOFC stack produces electrical power together with an exhaust stream that contains unused CO and H_2. The exhaust stream is routed to the shift reactors, where the CO reacts with H_2O to produce CO_2 and H_2. There is sufficient H_2O in the flow stream to allow most of the CO to be oxidized to CO_2. Beyond the shift reactors, the remaining traces of CO are removed by selective catalytic oxidation. This is necessary to prevent poisoning of the Pt catalysts used in the PEMFC stack. The resulting H_2-rich stream is cooled to about 70 °C before entering the PEMFC [18]. The fuel cells in Fig. 6 are connected in series for fuel feeding [58,59]. Using this configuration, the gas mixture fed to the cathode of the SOFC contains some water. However, the effect of water on cathode performance has not yet been fully understood, even though it is expected to degrade the electrode performance and to reduce the long-term durability of SOFCs. The true effect depends on the materials used for both the cathode and electrolyte [60]. The efficiency of the SOFC–PEMFC combination as predicted by simulations is about 60% [56,59]. The efficiency of the SOFC increases with operating pressure, but this has not been proven for the hybrid SOFC–PEMFC system [18]. By contrast, the efficiency of SOFC–PEMFC decreases with increasing operating pressures [18]. Yokoo et al. [59,61] presented a parallel fuel feeding configuration in which the reformed gas was separated into two flow streams for the SOFC and the PEMFC. In this parallel configuration, the PEMFC is fuelled from the reformer directly (unlike the serial configuration which uses depleted fuel from the SOFC anode). According to the study in Ref. [61], a 5% efficiency improvement was obtained with a parallel SOFC–PEMFC system as compared with the stand-alone SOFC.

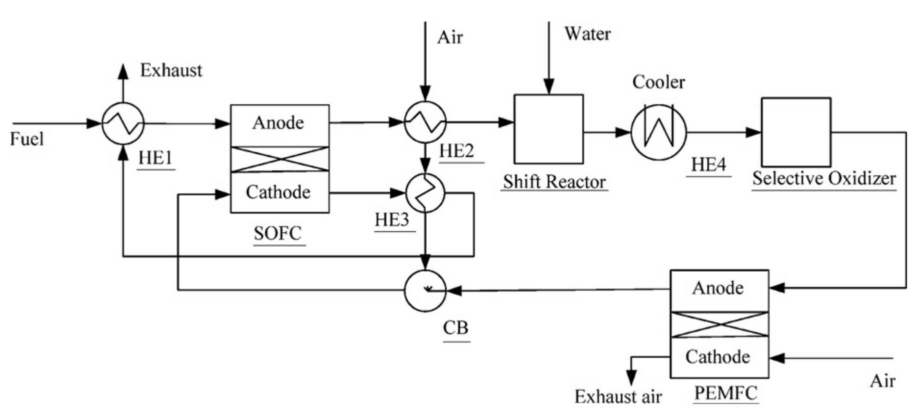

Fig. 6. Layout of an integrated SOFC–PEMFC system [18].

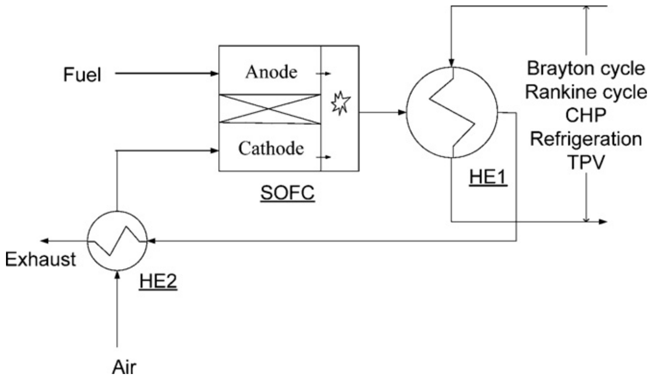

Fig. 7. Integration of a SOFC that uses indirect heat transfer.

3.2. Indirect thermal coupling scheme

An alternative thermal coupling scheme involves indirect heat transfer. As shown in Fig. 7, the indirect thermal coupling scheme includes two closed cycles. Aside from the SOFC cycle, the other closed cycle may be a thermal power generation plant (Rankine cycle, Brayton cycle or TPV) or a thermal utilization module (such as the combined heat and power (CHP) system with a refrigeration cycle). The two cycles operate at different pressures and with different working media. Often in the applications of CHP and refrigeration systems, the hot SOFC exhaust gas is first channeled to an air pre-heater HE2 and then to HE1 (see Fig. 7). This mainly depends on the operating temperature of the closed cycles.

3.2.1. SOFC + Brayton cycle (Rankine cycle)

Williams et al. [48] introduced a non-pressurized SOFC system combined with a Brayton cycle that uses a heat transfer scheme (see Fig. 8). Under this configuration, the fuel cell and the Brayton cycle each require their own independent air supplies. The fuel cell operates at atmospheric pressure and its hot exhaust gas is routed to heat the compressed air via a recuperator. The turbine exhaust gas passes through a heat exchanger to preheat the air before it enters the SOFC. According to the study reported in Ref. [48], this scheme yields lower efficiency than with direct coupling scheme. A maximum efficiency of around 45% can be obtained, which is 10% lower than that of the non-pressurized hybrid system [48]. The Rankine cycle is mainly used for stationary central power generation. More often, the SOFC is integrated with both Rankine and Brayton cycles [7,14,62–64].

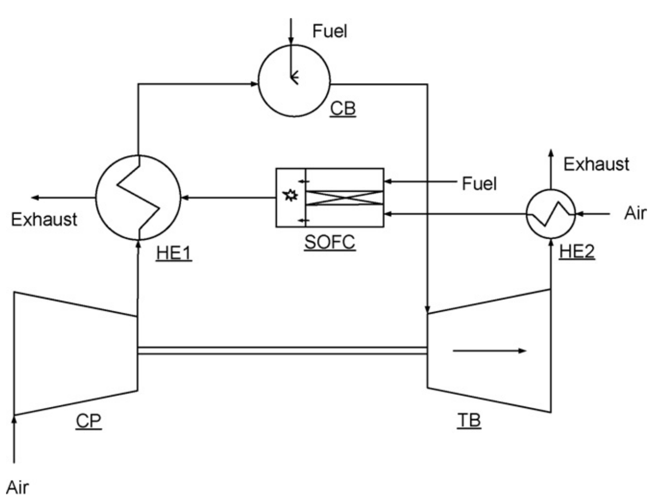

Fig. 8. Non-pressurized SOFC system combined with a Brayton cycle using a recuperator.

3.2.2. SOFC + CHP

In 2004, a demonstration unit featuring a SOFC-based 100-kW CHP system was launched by Siemens-Westinghouse [65–67]. The degradation of the generator stack was reported to be less than 0.1% per 1000 h of operation, with a life expectancy for the generator cells that is expected to be at least 40,000 h. In 2005, a 1 kW SOFC–CHP demonstration system was conducted in Japan at a residential house. The actual operation showed that this system made significant reduction in primary energy and CO_2 emission comparing with conventional energy supply modes [68].

Fig. 9 shows the basic configuration of a combined heat and power system. The technological and economic assessments have been conducted and are presented in many publications [69–73]. As shown in Fig. 9, the hot exhaust gas from the SOFC is first used to heat the inlet air of the fuel cell and is then sent to a heat exchanger to generate hot water. The Siemens-Westinghouse SOFC–CHP demonstration unit has reportedly achieved a 46% (LHV) net AC efficiency and 75% energy efficiency [26]. A small size 1-kW-class SOFC–CHP system can attain 44% (AC output, LHV) average electrical efficiency [68].

3.2.3. SOFC + absorption refrigeration cycle

Absorption refrigeration machines are widely used in residences and buildings for air conditioning. The absorption cycle is a process by which the refrigeration effect is created through the use of a refrigerant cycle and another working fluid cycle. The refrigerant cycle removes heat by evaporating the refrigerant at a low pressure and then absorbing it in lithium bromide water solution at a higher pressure. Some external heat is needed to drive the liquid refrigerant into a gaseous state in the vapor generator. The external heat is normally a side effect of industrial processes. In this context, the SOFC can be integrated with an absorption refrigeration cycle, which makes use of the exhaust SOFC thermal energy. Furthermore, the electrical power for the building can be tapped from the SOFC. Studies of this type of integration system have been reported in Refs. [19,70,74].

Absorption machines are commercially available today in two basic configurations. One machine, which uses lithium bromide (LiBr) as the absorbent and water as the refrigerant, is primarily for air conditioning applications above 0 °C. The other, which uses ammonia and water (with the former being the refrigerant and the latter the absorbent), is suitable for applications below 0 °C. Fig. 10 illustrates an integration cycle for the combined SOFC LiBr absorption refrigeration system. There are four closed cycles in the system: (1) the SOFC power generation cycle, (2) the condensing water cycle, (3) the chilled water cycle, and (4) the refrigerant cycle. The SOFC exhaust is channeled to the fuel cell inlet air recuperator and then routed to a vapor generator to heat the $LiBr/H_2O$ solution, thereby causing the refrigerant – in this case water – to be boiled out of the solution in a manner similar to distillation. Generally, we can add a heat exchanger downstream of the vapor generator to produce hot water that utilizes the exhaust heat. Zink et al. [19] studied a SOFC-based system that featured a cooling cycle and a heating cycle. The predicted net efficiency was better than 87%.

3.2.4. SOFC + thermophotovoltaic (TPV) power generation

The use of TPV power generation dates back to 1963, when the concept was proposed by Wedlock, but it was only practically implemented in recent years with strong support from the semiconductor industry and through the use of microfabrication technology [75–80]. One of the advantages of TPV is fuel flexibility, which makes it promising for the recovery of high-temperature exhaust gases from SOFCs.

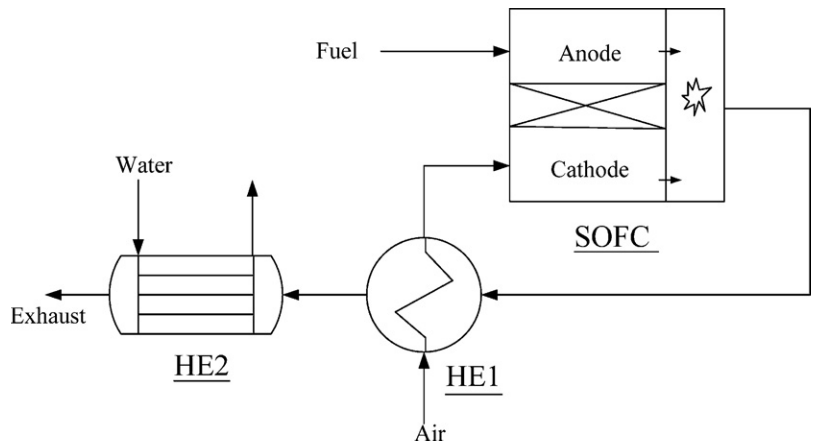

Fig. 9. Combined heat and power cycle of a SOFC.

TPV power generation operates on the principle of the photovoltaic effect, in which photons (whose energy is greater than the bandgap of the cell) can create electron–hole pairs [78]. Fig. 11 shows an integrated system that combines a SOFC with a cylindrical TPV power generation system. As shown in the internal configuration of the TPV in Fig. 11, the essential component is the combustion chamber where the unutilized fuel from the SOFC exhaust is incinerated. The combustor is surrounded by an infrared emitter that generates photons from the radiant energy emitted by the combustor. Depending on the emitter temperature, a filter is installed to improve TPV performance by selectively filtering out the thermal radiation. The filter transmits the above-bandgap photons to the TPV cell but reflects the sub-bandgap photons back to the emitter for recuperation. The TPV cells then convert the thermal radiative energy into electrical power. A cold air stream is routed to the channel between the TPV cells and the filter to prevent the cells from overheating. The emitter operating temperature in the TPV normally ranges between 1300 and 2000 K [81]. Today, the efficiency of the TPV is relatively low (<20%) due to the significant amount of unused radiation [82]. Therefore, the waste heat of the TPV can be further utilized by other thermal plants.

3.3. Fuel coupling scheme

As a key reactant in electrochemical contexts, hydrogen can be produced by various technologies (depending on the kind of feedstock fuel). Fig. 12 illustrates the fuel coupling scheme with various hydrogen production technologies. The steam reforming process normally uses natural gas. The coal gasification cycle produces syngas whose impurity is subsequently removed before it is fed to the SOFC. Coal gasification systems are regarded as one of the most important technologies for future large-scale centralized zero-emission power generation. Thermochemical water-splitting converts water into hydrogen and oxygen using a series of ther-

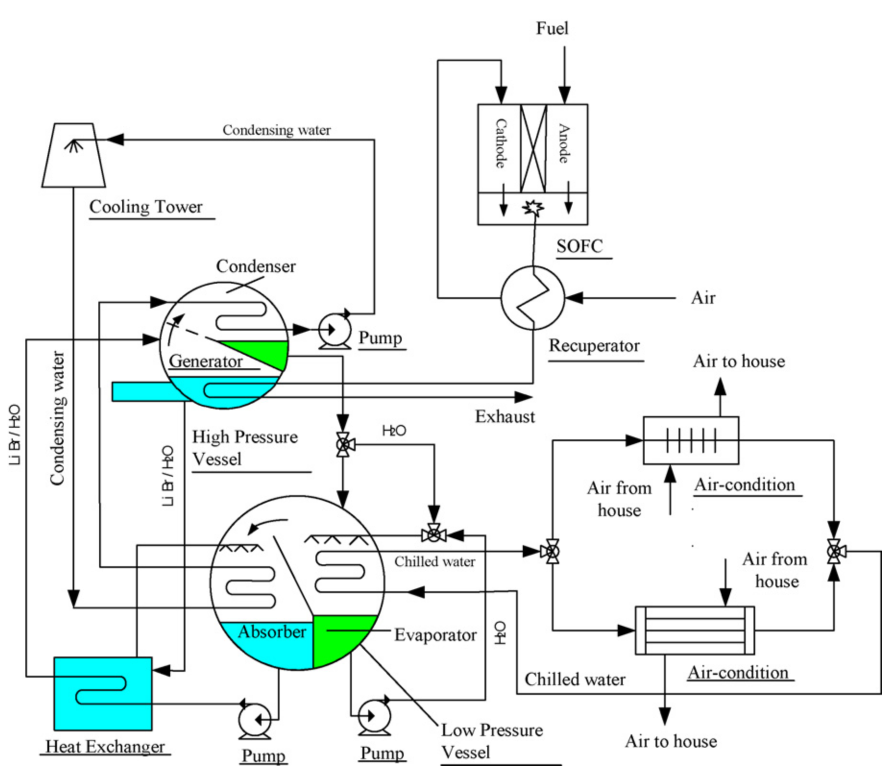

Fig. 10. Hybrid system consisting of a SOFC combined with an absorption refrigeration cycle.

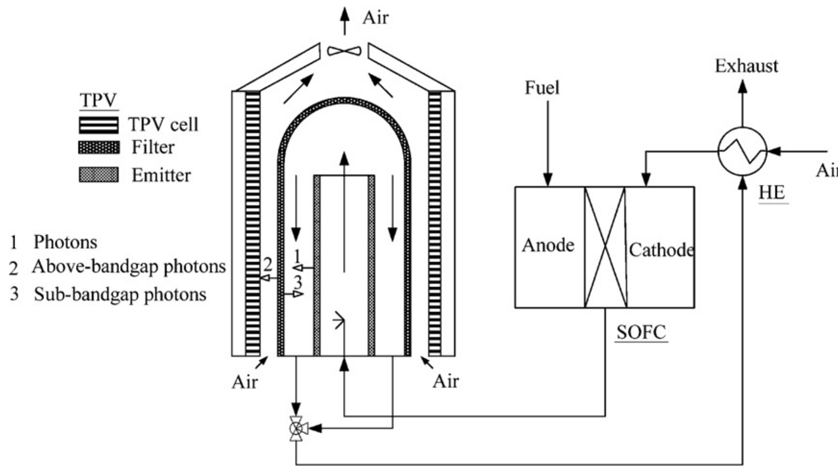

Fig. 11. Hybrid system consisting of a SOFC combined with thermophotovoltaic power generation.

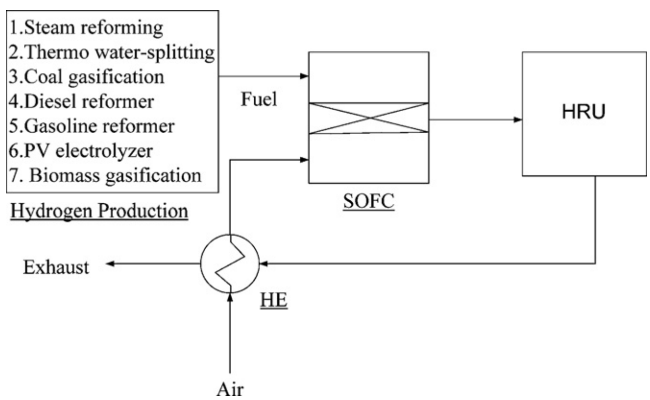

Fig. 12. Integration of a SOFC based on a fuel coupling scheme.

mally driven chemical reactions. Brown et al. [83] and Schultz [84] presented a concept to use a nuclear reactor as the energy source for thermochemical processes in order to produce hydrogen. A combined SOFC–nuclear reactor power generator has been proposed by Palmer [14]. By integrating a SOFC with a diesel reformer or a gasoline reformer, a SOFC can be adopted as an auxiliary power unit (APU) in automotive applications [85,86]. An electrolyzer is a device that converts water into hydrogen and oxygen. In the solar photovoltaic (PV) power system, the electrolyzer uses the excess electrical energy to produce hydrogen during the day. The stored hydrogen can be used to feed a fuel cell during the night [87,88]. Today, there exist three principal types of electrolyzer: alkaline, PEM and solid oxide. An integration power system involving a SOFC integrated with a solar PV, and an electrolyzer storage unit, was designed for aerospace applications [89].

3.3.1. SOFC + a hydrocarbon fuel ATR

Due to an increasing focus on convenience and safety, the use of engine-independent electricity has gained tremendous support in the area of automotive applications. The fuel cell APU can significantly improve the efficiency and quality of generated electricity, especially in low power demand scenarios. Both SOFCs and PEMFCs are good candidates for APU applications. However, the PEMFC requires ultra clean hydrogen reformates that need relatively complex cleanup processes for different temperatures. In the SOFC systems, the main components all operate at the same temperature. In particular, SOFCs can be fuelled by the infrastructure fuel (often diesel or gasoline) when it is integrated with a hydrocarbon auto-thermal reformer (ATR). Automotive suppliers, such as Delphi and Webasto AG, have designed APUs with SOFCs [16,90–92].

Fig. 13 shows a schematic configuration of a SOFC integrated with an auto-thermal reformer that is fuelled by diesel and gasoline. Studies of auto-thermal reforming have been widely reported [93–96]. The ATR reactor is the core fuel processing system, which combines the catalytic partial oxidation (CPO) and the steam reforming (SR) processes under thermoneutral conditions. It incorporates a catalyst bed, an injector/atomizer/mixer and a glow plug [94]. As shown in Fig. 13, the ATR-fed water is vaporized in a steam generator that utilizes the SOFC exhaust heat. The steam is mixed

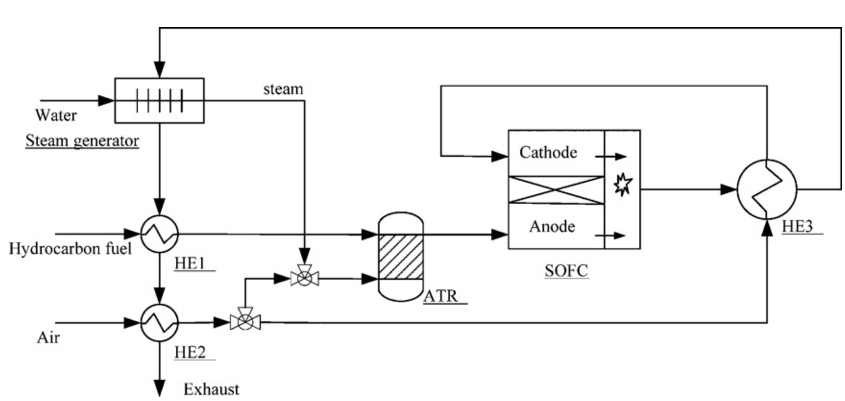

Fig. 13. Combined SOFC and auto-thermal reforming of hydrocarbon fuel.

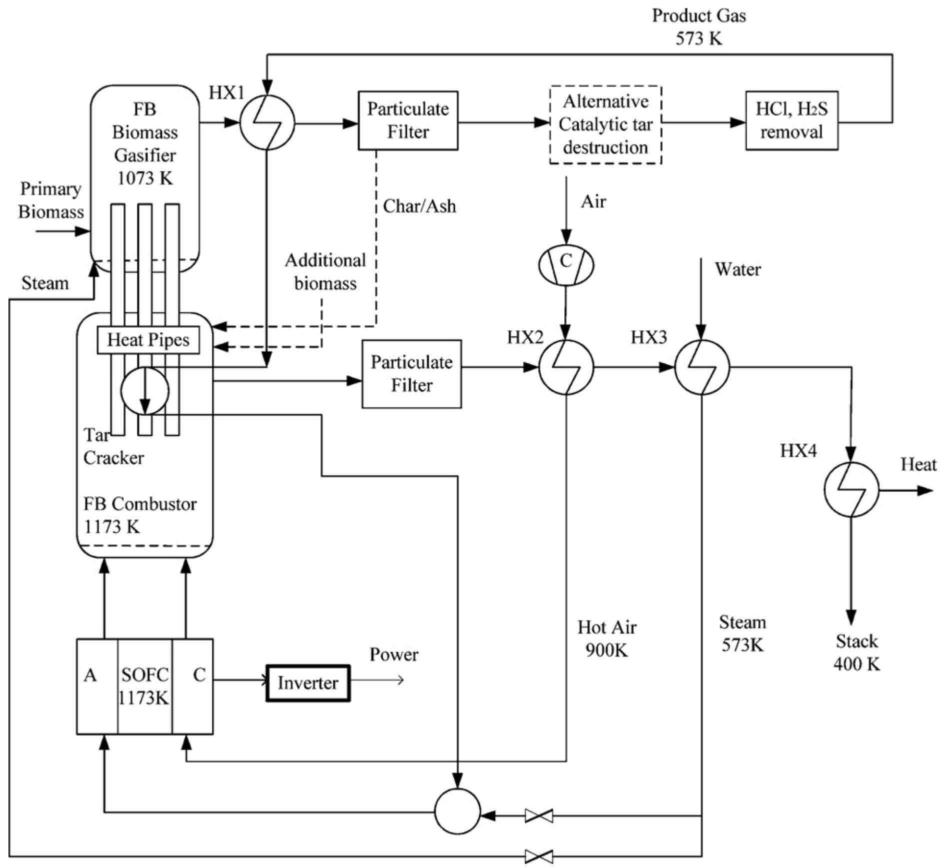

Fig. 14. Integration of SOFC with allothermal biomass gasification [105].

with air prior to entering the ATR. The liquid hydrocarbon fuel is evaporated via the injector and atomizer and is mixed with the humidified air in the ATR. The CPO and SR reactions as well as the thermal decomposition of hydrocarbon fuels in the presence of catalysts are as follows:

$$C_mH_n + \frac{m}{2}O_2 \rightarrow mCO + \frac{n}{2}H_2 \quad \text{(R7)}$$

$$C_mH_n + mH_2O \rightarrow mCO + (n/2 + m)H_2 \quad \text{(R8)}$$

$$C_mH_n \rightarrow mC + \frac{n}{2}H_2 \quad \text{(R9)}$$

The CPO reaction involving a sub-stoichiometric ratio of oxygen and hydrocarbon is weakly exothermal, and produces H_2 and CO (R7). The heat released is utilized by the endothermic steam reforming reaction (R8). The removal of coke deposition (R9) is described in more detail in Ref. [97]. In fact, the added steam in the air stream can suppress carbon formation via the following reaction:

$$C + H_2O \rightarrow CO + H_2. \quad \text{(R10)}$$

Since the depleted SOFC fuel contains significant H_2O, the steam supplement can be provided by recirculating part of the anode exhaust gas to the ATR [98]. Separately, SOFCs can also be integrated with a battery, thus creating an integrated power source for an electric automobile. Brett et al. [99,100] proposed a combined intermediate-temperature SOFC with a sodium-nickel chloride battery for automotive applications.

3.3.2. Biomass gasification + SOFC

Biogas is an attractive fuel source that is indigenous, local, versatile and renewable. However, it remains underexploited. The biomass gasification process would seem to be thermally compatible with SOFC because both operate within the same temperature range. The combination of SOFC with biomass gasification can significantly increase the value of the biogas. Gasification can be classified according to the type of gasifier (fluidized bed or fixed bed), operating conditions, gasifying agent, etc. Generally, gas produced by biomass gasification contains hydrogen, carbon monoxide, carbon dioxide, water vapor, nitrogen, methane and other heavier hydrocarbons and trace components. Different gasifying agents will result in different gas compositions and qualities of the resulting biomass. Air, oxygen and steam are usually used either individually or mixed together as a gasifying agent. If air or oxygen is used, the oxidation process itself should generate the heat that is necessary for the reactions; thus, no external heat energy supply would be needed. Air gasification produces gas products with a low heating value (typically in the range of 4–6 MJ Nm^{-3}) and an H_2 concentration of only 8–14 vol.% due to the significant amount of N_2 in the air (which dilutes the gas mixture) [101–103]. Oxygen and steam gasification would produce a improved heating value of about 10–18 MJ Nm^{-3} [104], but oxygen gasification requires a major investment in oxygen production equipment. Steam gasification is an attractive process, and produces gas with 35–45 vol.% of H_2 and 20–30 vol.% of CO [101].

Fig. 14 shows a flow chart for the combined SOFC–allothermal steam gasification CHPs [105]. The first step of biomass gasification is an immediate drying and thermal decomposition of solid fuel to generate light gases, tars and char. The pyrolyzed gases and tars then react with the gasification agent in the gaseous phase, whereas the solid char participates in several heterogeneous reactions with the gases:

$$C + CO_2 \leftrightarrow 2CO \quad (R11)$$

$$C + 2H_2 \leftrightarrow CH_4 \quad (R12)$$

$$C + H_2O \leftrightarrow CO + H_2 \quad (R13)$$

$$CH_4 + H_2O \leftrightarrow CO + 3H_2 \quad (R14)$$

$$CO + H_2O \leftrightarrow CO_2 + H_2 \quad (R15)$$

The proposed system operates at near-atmospheric pressure with two fluidized bed (FB) reactors that are thermally coupled using heat pipes. The gasifier and combustor operate at 1073 K and 1173 K, respectively; this temperature difference of 100 K allows for good heat transfer via the integrated heat pipes, which provide the thermal energy needed for allothermal gasification. The cleaned gas is reheated in HX1 and then channeled into a compact tar-cracking reactor that is within the FB combustion zone. The clean fuel gas is routed to the SOFC anode for power generation. Air is blown such that the pressure is near the operating pressure of the SOFC and is heated in HX2 before entering the stack. The depleted fuel and air from the SOFC are mixed and incinerated in the secondary FB together with the char, a gasification byproduct. Additional biomass may be provided if the above-mentioned materials are insufficient to sustain the gasification. The flue gas is recuperated in HX2 for heat extraction, and then enters a heat recovery steam generator (HRSG) HX3, which provides steam for the gasification and fuel gas moisturizing processes. HX4 offers useful heat in the form of hot water.

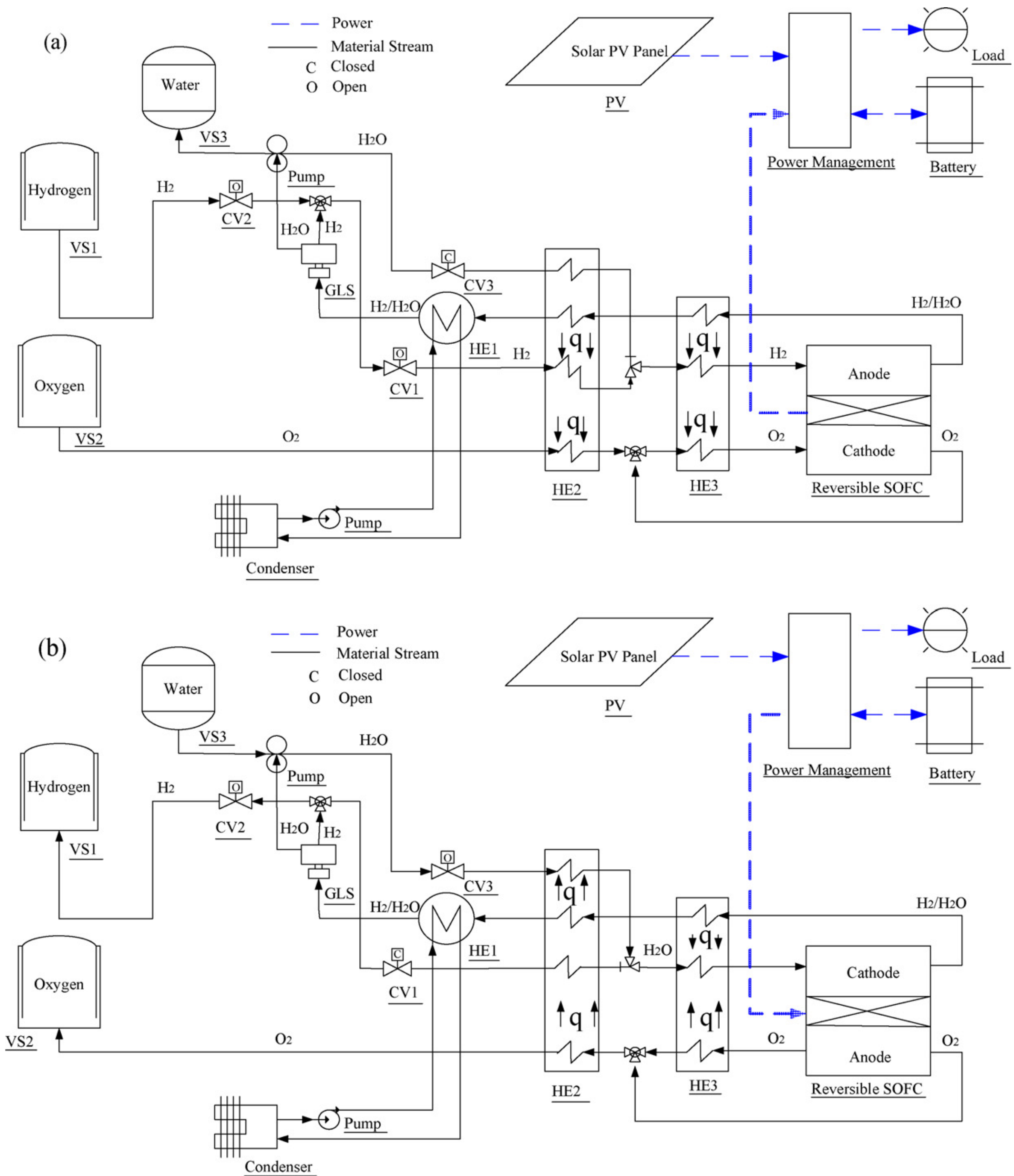

Fig. 15. Hybrid system comprising versatile SOFC and PV cell [89]: (a) SOFC mode and (b) SOEC mode.

Table 2
Typical SOFC integration strategies.

Configuration	Application	Energy source	Development status
Steam reformer + SOFC + Brayton cycle + Rankine cycle	Central power generation; ship	Natural gas	Concept
Thermochemical hydrogen production + SOFC + Brayton cycle + helium Brayton cycle	Naval vessel; central power generation	Nuclear reactor	Concept
Coal gasification + SOFC + Brayton cycle + Rankine cycle	Central power generation	Coal	Concept
SOFC + Brayton cycle	Distributed power generation	Natural gas	Demonstration [26,47]
SOFC + Brayton cycle + Cheng cycle	Distributed power generation	Natural gas	Concept
SOFC + CHP	Distributed power generation; building	Natural gas	Demonstration [26,68]
SOFC + refrigeration cycle	Building	Natural gas	Concept
SOFC + TPV	Distributed power generation; aerospace	Natural gas	Concept
Electrolyzer + SOFC + PV	Aerospace; distributed power generation	Solar energy	Concept
Gasoline reformer + SOFC	APU for automobile; APU for airplane	Gasoline	Demonstration [90]
Diesel reformer + SOFC	APU for automobile	Diesel	Demonstration [92]
Biomass gasification + SOFC	Distributed power generation	Biomass	Concept

An energy analysis suggests that the electrical efficiency of the above-mentioned system is about 32%, while the thermal efficiency is 35% when olive kernel residues are used as biomass [105]. Modeling the bio-derived gas utilization in SOFCs predicts efficiencies in the range of 23–50% [101,106–108]. Simulation results also suggest that the electrical efficiency exhibits a positive dependence on the hydrogen content of the biomass feedstock [103]. The combination of a SOFC/GT and biomass gasification was also investigated [109,110]. An integrated pressurized gasifier with a SOFC/GT system can reach an electrical efficiency of 41% while the combination of an atmospheric gasifier and a SOFC gives 20% electrical efficiency [109]. The gasifying agent may also impact performance. The work of Sucipta et al. [110] showed that a steam biomass gasification system may offer higher efficiency than an oxygen and air gasification system.

3.3.3. Reversible SOFC + PV

The photovoltaic (PV) cell is a device that converts solar energy into electrical energy. It is widely used as a power generation plant in remote areas and on board spacecraft. The power output of a PV cell is highly time-dependent, and acts as an energy source with varying intensity. There is a need to store excess energy during the day. Batteries are the most commonly used storage device for this purpose; however, they typically are appropriate for short-term applications [111]. Hydrogen is considered to be a more promising medium due to recent technological advancements in electrolyzers and fuel cells. The integration of PV cells and PEMFCs with low-temperature electrolyzers (alkaline and polymer membrane) has been studied by many researchers [111,87,112–116]. Compared to the low-temperature electrolyzer, the high-temperature solid oxide electrolyzer offers a higher efficiency and longer-term stability and can operate at higher pressures. This type of electrolyzer has received increasing attention in recent years [117–123].

A versatile SOFC includes two modes of operation: (1) as a solid oxide fuel cell for power generation, and (2) as a solid oxide electrolysis cell (SOEC) for hydrogen production. Fig. 15 shows a system that features a versatile SOFC and a solar PV cell, which meets the relevant load requirement through the power management unit. The excess electrical power is stored in a battery for the short term or is supplied to a versatile SOFC for hydrogen production purposes. In the SOFC mode (Fig. 15(a)), hydrogen from VS1 is fed to the anode and oxygen is transferred from VS2 to the cathode of the SOFC. Hydrogen reacts with oxygen ions to form water and release heat (Fig. 1). The generated power is transmitted to an electrical load or is stored in a battery through the power management unit. The anode outputs a mixture of H_2 and H_2O. The exhaust heat is utilized in HE2 and HE3. The H_2/H_2O stream is further cooled by HE1 and is separated in a gas–liquid separator (GLS). The liquid water is routed to VS3 and hydrogen is recirculated. The control valve CV3 is closed in the SOFC mode. In the SOEC mode (Fig. 15(b)), the operation is the reverse of the fuel cell mode; electrons are injected into the cathode by an external power supply, which may either be the solar PV cell or the battery via the power management unit. This forces oxygen ions (from H_2O) to migrate through the electrolyte from the cathode to the anode. The reactions are as follows:

$$\text{At the cathode side}: \quad H_2O + 2e^- \rightarrow H_2 + O^{2-} \tag{R16}$$

$$\text{At the anode side}: \quad O^{2-} \rightarrow (1/2)O_2 + 2e^- \tag{R17}$$

$$\text{The net electrolysis reaction is}: \quad H_2O \rightarrow H_2 + (1/2)O_2 \tag{R18}$$

A significant part of the heat required for the electrolysis process is obtained from the irreversible losses caused by the electrolysis reaction and the passage of an electric current through the cell in conjunction with relevant activation, concentration and resistance overpotentials. This reduces the overall electricity consumption [124]. The exhaust heat is utilized in HE2 and HE3 to vaporize the liquid water.

4. Advanced integration cycles for improved power generation

Three basic integration strategies were introduced above to build the integration system based on SOFCs. Quite often, the integration system can be configured using more than one scheme. Table 2 lists typical conceptual integration strategies that use SOFCs. In this paper, we review three advanced conceptual integration systems – the SOFC is integrated with a gas-cooled nuclear reactor cycle, coal gasification cycle, and humid air turbine cycle power generator.

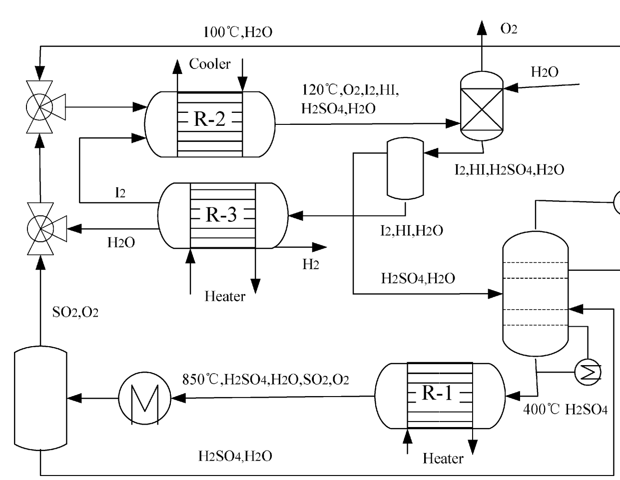

Fig. 16. Sulfur–iodine cycle of hydrogen production involving thermochemical water-splitting [126].

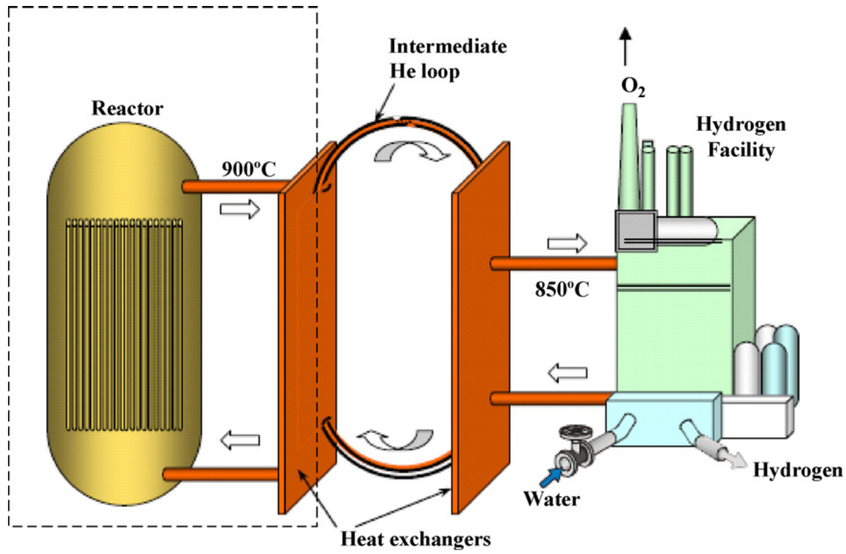

Fig. 17. Sketch of a nuclear reactor heat source with water-splitting hydrogen production by thermochemical processes [127].

4.1. SOFC + MHR + helium turbine + gas turbine

Hydrogen is a clean energy carrier that produces no pollution or greenhouse gas emissions when it is oxidized. It is very important to develop hydrogen production infrastructures that support the hydrogen economy. Recent hydrogen production technology has focused on fossil fuels and, more specifically, on natural gas. When hydrogen is produced using energy derived from fossil fuels, there is little or no environmental advantage. Currently, there is no large-scale, cost-effective, environmentally attractive com-

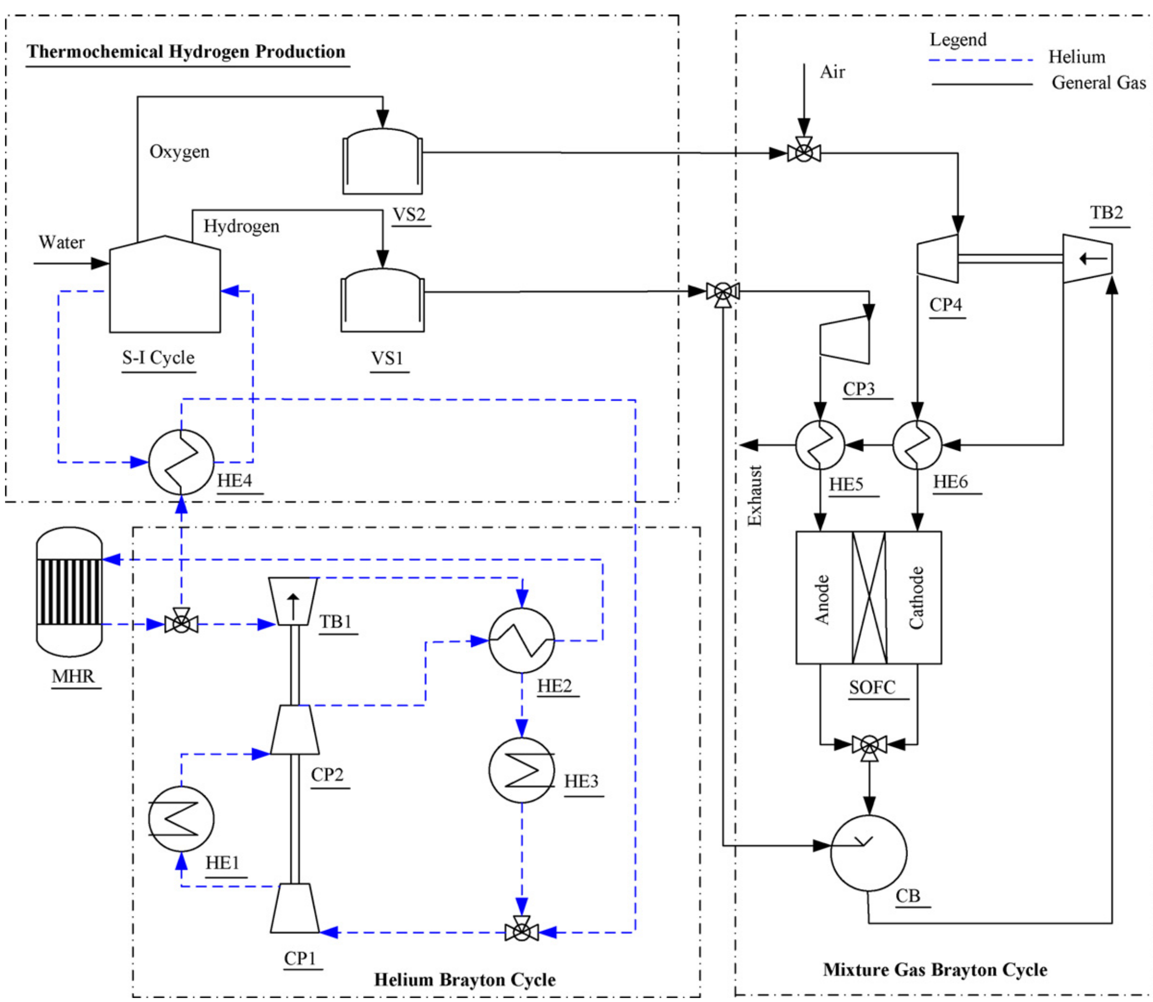

Fig. 18. Integration scheme for a SOFC and modular helium nuclear reactor that uses thermochemical hydrogen production.

mercialized hydrogen production process, nor has such a process been identified. Some researchers have addressed the possibility of using thermochemical processes to create hydrogen using an advanced high-temperature nuclear reactor as the primary energy source [83,84]. Thermochemical water-splitting is a chemical process that decomposes the water into hydrogen and oxygen using only heat or, in the case of an integrated thermochemical process, by a combination of heat and electrolysis, which may meet the above goals. The sulfur–iodine (S–I) cycle is one of the prime thermochemical processes studied. The chemical reactions are as follows [83,125,126]:

$$H_2SO_4 \rightarrow SO_2 + H_2O + 0.5O_2 + 44.348\,\text{kcal mol}^{-1}\,(850\,^{\circ}\text{C}) \quad \text{(R19)}$$

$$I_2 + SO_2 + 2H_2O \rightarrow 2HI + H_2SO_4 - 52.626\,\text{kcal mol}^{-1}\,(120\,^{\circ}\text{C}) \quad \text{(R20)}$$

$$2HI \rightarrow I_2 + H_2 - 4.21\,\text{kcal mol}^{-1}\,(450\,^{\circ}\text{C}) \quad \text{(R21)}$$

$$H_2O \rightarrow H_2 + (1/2)O_2 \quad \text{(R22)}$$

Note that the reactants H_2SO_4 and I_2 other than water are regenerated and recycled through the reactions. Reaction (R19) is highly endothermic, reaction (R20) is very exothermic, and reaction (R21) is slightly endothermic.

The S–I cycle is illustrated in Fig. 16. The cycle uses only energy (in the form of heat) and water as inputs. The only products are hydrogen and oxygen and some rejected heat. The efficiency of this cycle is predicted to reach 45–50% [127]. The Japan Atomic Energy Research Institute (JAERI) has successfully conducted continuous production experiments using the S–I cycle. JAERI is developing the process as part of a program aimed at integrating it with a high-temperature gas-cooled reactor (HTGR), using helium as the coolant [126].

Fig. 17 shows a hydrogen production system that functions by combining thermochemical water-splitting with thermal energy from a nuclear reactor. It is important to determine the type of reactor that should be used. Some attributes of the reactor and criteria should be considered such as coolant stability, chemical compatibility, pressure requirements, nuclear requirements, etc. Many of the current commercial operating nuclear power plants are of second-generation or third-generation pressurized water reactors (PWRs) and boiling water reactors (BWRs) [128]. Nine basic types of reactor were assessed by Marshall on account of their significant design, safety, operational and economic issues [129]. A typical modular high-temperature gas-cooled reactor (HTGR) appears to be appropriate as a heat source for S–I cycle applications. The modular helium reactor (MHR) and associated gas turbine utilize helium as both the fluid that removes heat from the reactor and the working fluid for the gas turbine's Brayton cycle. As shown in Fig. 17, helium is also used as an intermediate fluid for the exchange of heat between the primary coolant cycle and the S–I cycle.

Fig. 18 presents the schematic integration strategy for a SOFC and a gas-cooled nuclear reactor given a thermochemical hydrogen production cycle. Three primary cycles, including a hydrogen production cycle and two Brayton cycles, are integrated in this system. The heat source for the S–I cycle (as shown in Fig. 17) is provided by the MHR through a closed heat exchange cycle. The coolant system for the nuclear reactor involves a Brayton cycle, which uses water as the coolant to remove heat from the reactor and to run the steam turbine's Rankine cycle. The resulting hydrogen and oxygen are stored in VS1 and VS2. The hydrogen is supplied to a SOFC and is used as auxiliary fuel for the combustor CB.

Table 3
Typical composition of gasified fuel [132].

H_2	25–30%
CO	30–60%
CO_2	5–15%
H_2O	2–30%
CH_4	0–5%
H_2S	0.2–1%
COS	0–0.1%
N_2	0.5–4%
Ar	0.2–0.1%
NH_3 + HCN	0–0.3%

The integration strategy mentioned above is especially suited for naval vessels. We note that, although the addition of a SOFC in a nuclear power system improves the overall efficiency of the cycle, the main advantage of employing a SOFC is its high reliability, which is essential for the "all electric" naval vessel concept as well as for stable maneuverability and a relatively high efficiency (in the case of partial loading operations). Moreover, the SOFC reduces the size of the turbine, which can greatly reduce the vibration and noise of the vessel. Furthermore, the thermal energy of the MHR is used to generate hydrogen for the fuel cell, thus reducing the cost. Palmer [14] investigated an integration system that features a MHR combined with a SOFC fuelled by natural gas. The simulation results suggest that the system should approach an electrical efficiency of more than 60% [14].

4.2. SOFC + coal gasification + gas turbine + steam turbine

The FutureGen program launched by the U.S. DOE [7] aimed to develop and demonstrate advanced power plants that are highly efficient and effectively mitigate the environmental impacts associated with the use of fossil fuel. The conceptual designs for the FutureGen plant must meet the targets of Vision 21st [3]. The electrical efficiency of coal-based power generation is believed to be 60%. The integration system of a SOFC combined with coal gasification as well as a Brayton cycle and Rankine cycle is an alternative configuration that may be used to achieve the targets of Vision 21st [7,130,131].

The integration scheme features two islands, known as the coal gasification island and the power island. The coal gasification island produces the clean syngas for power generation plants. The power island includes the SOFC power generation cycles, gas turbine (Brayton cycle) and steam turbine (Rankine cycle). The auxiliary plants include a water treatment plant, air separation unit (ASU) and CO_2 sequestration system. The coal gasification process is used to convert the feedstock coal into syngas consisting of a mixture of carbon monoxide (CO) and hydrogen (H_2) and, to a lesser extent, some carbon dioxide (CO_2) and traces of other gases. The syngas is cleaned of particulates, sulfur and other contaminants. Fig. 19(a) illustrates all the processes and plants, including the coal gasification process, the particulate removal and recycling process, the raw syngas cooler, the acid gas cleanup (H_2S and COS removal and sulfur recovery), the zinc oxide polisher and the water treatment zone.

As shown in Fig. 19(a), the combustible constituents of the feedstock coal are partially oxidized by either air or pure oxygen in the gasifier. The products of gasification include carbon monoxide, hydrogen and a small amount of carbon, which is completely oxidized to yield CO_2 as well as a small amount of methane. The typical composition of gasified gas is shown in Table 3. The coal gasification processes operate at high temperatures and the associated heat recovery is effective at increasing the overall system efficiency. The raw syngas passes through a gas cooling zone, which is essentially a series of heat exchangers. The recovered heat is used to create steam, which is sent to the HRSG of Rankine cycle for superheating

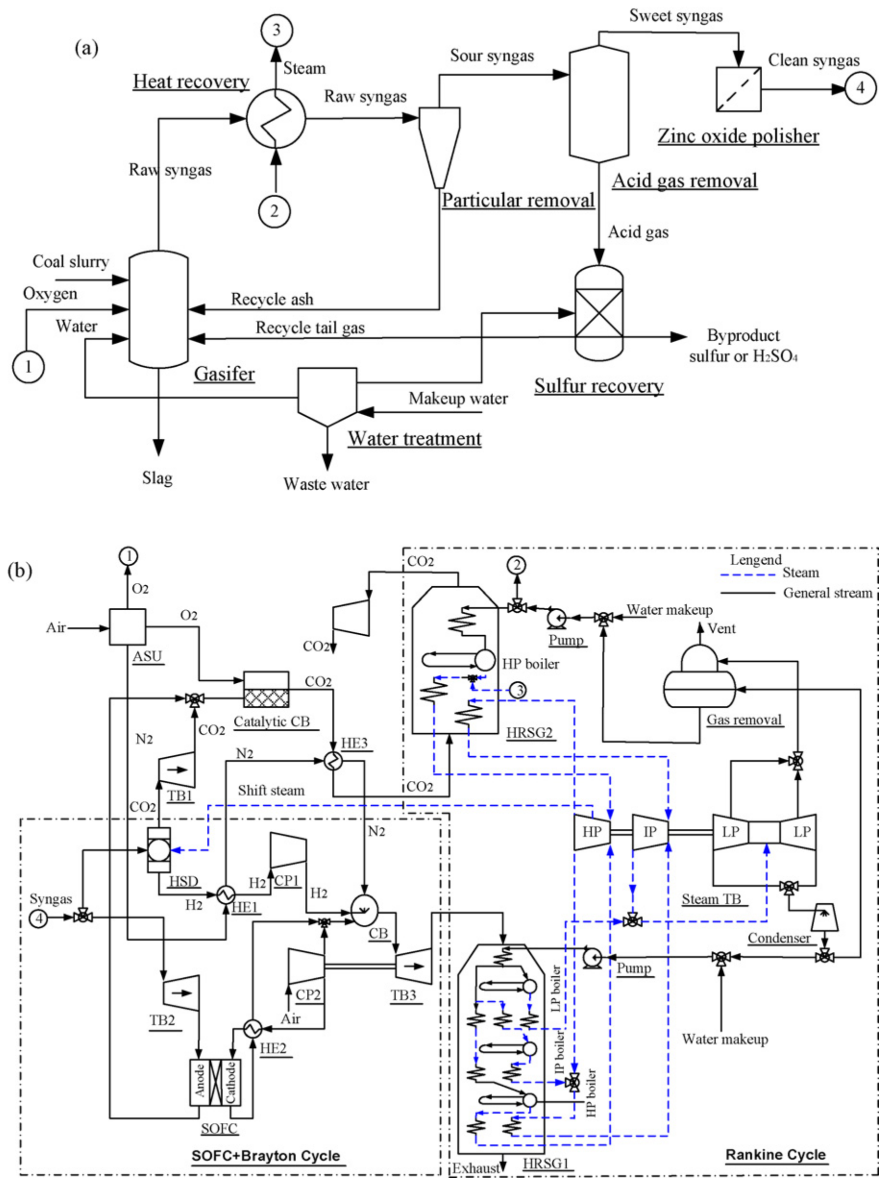

Fig. 19. Integration scheme for a SOFC and coal gasification system with carbon dioxide sequestration: (a) coal gasification island and (b) power island.

and reheating. The syngas exiting the gasifier is treated through a series cleaning devices for removing the particulates, carbonyl sulfide (COS), hydrogen sulfide (H_2S) and sulfur before entering the SOFC + Brayton cycle [132,133].

The power island is a power generation system that includes a SOFC module together with a Brayton cycle and a Rankine cycle (Fig. 19(b)). The clean syngas from the coal gasification island is separated into two gas streams. One is routed to the hydrogen separation device (HSD), which shifts the coal syngas and separates out a high purity hydrogen stream. The other syngas stream will first expand through the turbine TB2 before being transported to the SOFC as fuel. The anode exhaust stream of the SOFC, which contains rich CO_2 with small amounts of CO and H_2, together with the stream of CO_2 from the HSD, are sent to a catalytic combustor for reducing NO_x formation. Both the H_2 and CO are also combusted in a catalytic combustor. The high-temperature rich CO_2 stream from the catalytic CB is routed to the HRSG2 to produce and reheat the steam for the Rankine cycle. The hydrogen separated by HSD is supplied to the Brayton cycle. Nitrogen is recycled from the air separation unit (ASU) to the combustor of the Brayton cycle after being preheated in two heat exchangers. The exhaust of the gas turbine is used to produce steam in HRSG1. In the Rankine cycle, steam produced by HRSG is used to drive the turbines (HP, IP and LP).

Three cases dealing with the integration of a SOFC with a Brayton cycle and Rankine cycle based on coal gasification were studied by Parlsons et al. [7]. For cases involving no CO_2 capture, the efficiency obtained from the simulation was 56.4% for the hot gas cleanup method (with zinc oxide polisher) and 57% for the cold gas cleanup method. For the case of CO_2 capture, an efficiency of 49.7% (lower than that for the cases without CO_2 capture) was achieved due to additional power consumption in the process of CO_2 separation. Similar results were obtained by Rao et al. in Ref. [130] using a simulation method. The overall efficiency increases with increasing SOFC power output.

4.3. SOFC + humid air turbine (HAT) cycle

The humid air turbine (HAT) cycle has been proposed and studied for a number of years as a means of reducing cost when compared to combined cycles (CC). The integrated SOFC–HAT system was proposed by Rao and Kuchonthara in 2003 [63,134].

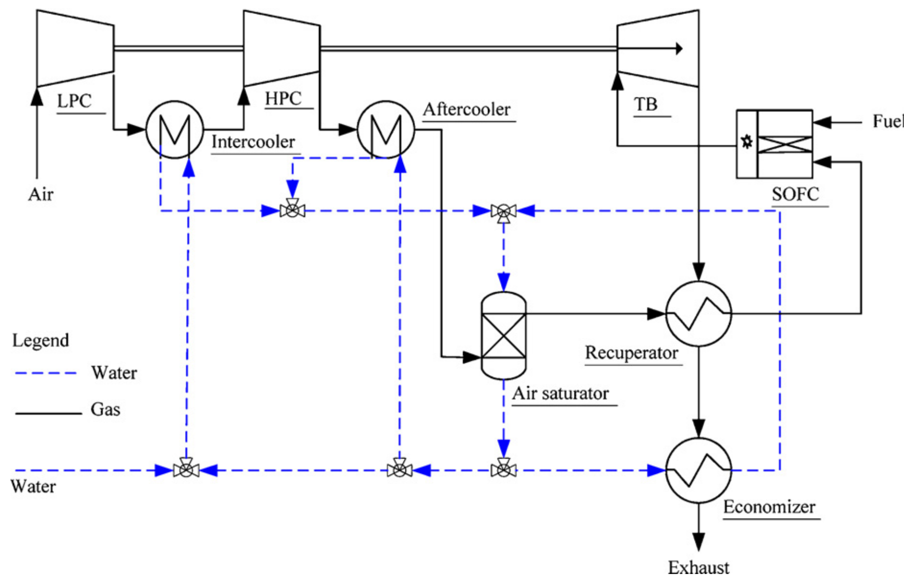

Fig. 20. Hybrid cycle for a SOFC combined with HAT.

Fig. 20 depicts the combined SOFC and HAT cycle. A typical HAT cycle operates in high-pressure ratio gas turbines. The air compression system includes a low-pressure compressor (LPC) and a high-pressure compressor (HPC) with an air intercooler. As shown in Fig. 20, the high-pressure air from the HPC is cooled in an aftercooler using cold water. In the air saturator, the pressurized air is humidified by bringing it into direct contact with hot water, which comes from the intercooler, aftercooler and economizer. The water leaving the air saturator is recirculated to recover the low-temperature heat from the intercooler, aftercooler and economizer. The humidified air is heated in the recuperator before entering the SOFC cathode. The unutilized fuel in the SOFC is first combusted and the product gas expands through the turbine (where mechanical work is produced). The turbine can also be separated into two stages if the pressure ratio is too high. As reported in Ref. [134], one can add a low-pressure SOFC module or combustor between the two expanders. The fuel for the SOFC can be either natural gas or syngas.

Compared to a combined cycle, the efficiency of the HAT cycle is typically lower by several percentage points, but it has the advantage of offering lower cost. Eliminating the HRSG/steam sub-cycle in the HAT cycle reduces the cost, which more than compensates for the added expense of a sophisticated gas turbine, an air saturator and a few heat exchangers [7]. The simulation results from Rao and Samuelsen [134] show that the efficiency of the SOFC–HAT integration cycle can be as high as 69.05% (LHV) while running on natural gas at a pressure ratio of 15. A potential disadvantage associated with this cycle is that the partial pressure of the oxygen in the air stream entering the SOFC is reduced, which decreases the Nernst potential and the mass transfer rate of the oxygen through the cathode and increases the cathode concentration and activation polarizations.

5. Conclusions and final remarks

5.1. Achievements

SOFC power systems can be classified into three groups: stationary applications – including central power generation (>50 MW) and distributed power generation (usually >10 kW), APUs in vehicle applications, and portable applications. Most of today's installed SOFC units for demonstration purposes are at the sub-MW level. These units are mostly found in Europe, North America and Japan. The success of SOFCs and integrated systems in terms of possible future commercialization depends on their cost and efficiency. SECA has designed and manufactured several SOFC prototypes, which range from 3 to 10 kW. The projected system operational cost is in the range of $724–775 per kW [135].

The best-known tubular SOFC was developed by Siemens-Westinghouse. A 100 kW SOFC–CHP system fed with natural gas has been operating successfully at atmospheric pressure with an efficiency of 46% for over 29,000 h in the Netherlands, Germany and Italy [67]. A similar scaled-up 250 kW SOFC–CHP system built by Siemens-Westinghouse has been operating at a Kinetrics Inc. Facility in Toronto, Canada. These atmospheric SOFC–CHP systems, with electrical efficiencies in the range of 45–50%, are expected to be the initial commercial products of Siemens-Westinghouse [136]. Siemens-Westinghouse also offers two other proof-of-concept demonstrations of pressurized SOFC/GT hybrid systems, namely a 220 kW unit at the National Fuel Cell Research Center in Irvine, CA and a 300 kW unit in Pittsburg, PA. Rolls-Royce is developing a 1-MW hybrid system of pressurized SOFCs and gas turbines for stationary power generation. In Japan, Mitsubishi Heavy Industries (MHI) successfully installed a 200-kW hybrid system featuring SOFC–GT technology in 2006. Recently, several developers of SOFCs in Europe made progress on new prototypes and field trials. Ceramic Fuel Cells Ltd. (CFCL) signed an agreement with utility E.ON UK to develop and deploy a prototype SOFC–CHP unit in Britain. Ceres Power, which is developing intermediate-temperature SOFCs, has designed and built an integrated, wall-mountable CHP unit. Hexis has reported successful testing of its Galileo 1000 N SOFC heating systems with several large energy suppliers in Switzerland and Germany since 2007 [137].

5.2. Challenges

(1) *Cost reduction*. Although there remain several important technical hurdles to be resolved, the key to the future commercial

success of SOFC systems will be economic. Today, the most widely deployed fuel cells cost about US$4000–8000 per kW; by contrast, a diesel generator only costs US$800–1500 per kW, and a natural gas turbine can be US$400 per kW or less. The cost of SOFC stacks depends mainly on the materials and fabrication techniques employed. Due to high operating temperatures, most of today's SOFC systems use expensive materials. Some researchers maintain that low operating temperatures are necessary and that low cost metals could be used as interconnectors and for gas manifolding. However, the electrolyte resistance and electrode reaction kinetics are both impaired when the operating temperature is reduced. Currently, the cost of manufacturing constitutes the largest fraction of the total cost of the SOFCs. The well-known tubular SOFC developed by Siemens-Westinghouse was fabricated using an expensive electrochemical vapor deposition (EVD) process. The manufacturing technologies must be improved to offer increased yield. Some additional cost reduction can be achieved with improved power densities.

(2) *SOFC module scale-up*. For stationary power generation, the SOFC capacity ranges from kilowatt to megawatt levels. In order to reduce the manufacturing cost, vendors usually develop their nominal stacks of SOFC modules for mass-customization according to the different power rating requirements. Today, only SOFCs in the range of hundreds of kW have been demonstrated for tubular cells. Scaling the SOFCs up to the MW scale has yet to be demonstrated. The challenges arise in the scale-up step that focuses on the stack design, system layout, materials and configuration for long-life operation, manufacturing method, cell performance, thermal energy management, mechanical stress and the state-of-the-art BoPs.

(3) *Diagnostic, safety and control system*. The safety and reliability of operations must be ensured during deployment. Furthermore, integrated systems are more complicated than stand-alone SOFCs. Coupling, in terms of the exchange of both thermal energy and material between the components in the integration system, should be holistically assessed. System control issues have been addressed by several research groups [138–147]. The challenges need to be overcome in order to guarantee operation under practical conditions. The control strategies and configurations as well as related dynamic simulations have to be strengthened and validated using new demonstrations.

(4) *Large-scale hydrogen production*. Hydrogen is ideal to power the fuel cell. A hydrogen economy will likely reduce our dependence on fossil energy and decrease both toxic emissions and greenhouse gases. At present, about 95% of the H_2 used in the world is made from steam reforming of natural gas, and the remainder is produced by electrolysis, which is an energy-intensive route for splitting water into H_2 and O_2. The cost of using hydrogen in fuel cells is too high. More effort has to be put into the technological advancement of high-temperature electrolysis, thermochemical cycles and hydrogen storage in order to achieve major cost reductions.

(5) *CO_2 sequestration and capture*. Fossil fuels will continue to dominate our energy supply needs in the foreseeable future. The emission of carbon dioxide is believed to be the main contributor to the greenhouse effect. CO_2 capture can be employed favorably in both central power generation and distributed power generation contexts. Studies of SOFCs with CO_2 capture have been performed earlier by many researchers [148–150]. Three proposed methods, namely pre-fuel cell CO_2 capture, post-fuel cell CO_2 capture and post-fuel cell oxidation, were presented by Dijkstra and Jansen [150]. In most of these concepts, chemical and physical processes were adopted in the treatment of CO_2 sequestration and capture. Various high-temperature membranes can also be employed during the process of power generation via CO_2 capture [151]. However, intensive study is required to make cost-effective technologies for CO_2 sequestration and capture a reality.

(6) *Advanced turbine system* (*ATS*). The cost and performance characteristics of an ATS make it competitive for electric power generation and make possible cogeneration options in SOFC integration systems. To achieve a higher efficiency and lower emissions (consistent with the Vision 21st goals), turbine performance has to be enhanced significantly. In reality, the goal to achieve a higher turbine efficiency is in conflict with the goal of lower emissions. A higher working fluid temperature is necessary for higher efficiency, which implies that NOx emissions will be higher. However, limiting oxygen in order to lower NOx emissions can lead to unacceptably high levels of carbon monoxide and unburned hydrocarbon emissions. Furthermore, increasing the system temperatures would significantly challenge the materials scientists.

5.3. Future prospects

(1) *Pressurized SOFC + gas turbine*. This hybrid system offers advantages for distributed power generation (DG). Today, electrical energy mainly depends on central power generation. Central power generation offers excellent economies of scale, but usually transmits electricity over long distances, thus losing some of its energy. Furthermore, the waste heat cannot effectively be utilized because these power stations are usually distant from customers. The concept of DG reduces the amount of energy that is lost in transmitting electricity. As an attractive alternative to DG, the integration of a SOFC and gas turbine offers a solution for primary power that can augment the grid in ways that improve both efficiency, reliability and environmental impact.

(2) *SOFC + LiBr absorption refrigeration* (*and CHP*). A good air conditioning system is one of the key features of energy-saving buildings. Today, the heat sources for most absorption refrigeration systems are oil, natural gas or steam. The SOFC integration system, which combines heat, power and cold, will be more attractive to building services designers.

(3) *SOFC + ATR as APU for vehicle applications*. An APU provides electrical power independent of the drive system for a variety of automobile applications. The demand for electricity increases with increasing demand for convenience and safety, as well as for control and regulatory services. Examples of these functions include engine-independent air conditioning in automobiles or by-wire technologies in aircraft. Due to impressive efficiencies and environmentally friendly specifications, a SOFC-based APU with ATR is a good candidate for future applications.

(4) *IGFC*. Coal is still the main energy source that supports economical development in the foreseeable future. SOFC coal-based systems are expected to reduce both energy use and the environmental impact of energy production in the future.

(5) *SOFC + MHR*. The concept behind the SOFC + MHR system is to make use of a nuclear energy heat source to produce hydrogen by means of a thermochemical water-splitting process. Due to the synergistic effect of SOFC and MHR, the efficiency and stability of the power source is greatly improved. Specifically, in naval vessel applications, this system meets the requirements of the "all electric" concept, which effectively corresponds to being quiet, clean, and reliable.

Acknowledgement

This study was financially supported by the Doctor Foundation (No. DFXJTU2005-01) of Xi'an Jiaotong University.

References

[1] Environment Matters: Annual Review 2005. The International Bank for Reconstruction and Development, The World Bank, NW, 2005.
[2] National Energy Policy, Report of National Energy Policy Development Group, Washington, 2001.
[3] Vision 21 Program Plan-Clean Energy Plants for the 21st Century, U.S. Department of Energy, 1999.
[4] Institutional Plan-FY 2003–2007. U.S. Department of Energy, Office of Fossil Energy, National Energy Technology Laboratory, WV, 2002.
[5] U.S. Department of Energy, Office of Fossil Energy, National Energy Technology Laboratory, WV, Fuel Cell Handbook, 6th ed., EG & G Technical Services, Inc., Science Applications International Corporation, 2002.
[6] M.C. Williams, Fuel Cells 1 (2007) 78–85.
[7] E.R. Parlsons, W.W. Shelton, J.L. Lyons, Advanced fossil power systems comparison study-final report. U.S. Department of Energy, Office of Fossil Energy, National Energy Technology Laboratory, WV, 2002.
[8] C. Song, Catal. Today 77 (2002) 17–49.
[9] M.C. Williams, J. Strakey, W. Sudoval, J. Power Sources 159 (2006) 1241–1247.
[10] J.E. Freeh, J.W. Pratt, J. Brauwer, Proceedings of ASME Turbo Expo 2004, Vienna, Austria, 2004 (GT2004-53616).
[11] J.E. Freeh, C.J. Steffen, L.M. Larosiliere, Fuel Cell, 2005 (2005-74099, NASA/TM 2005-213805).
[12] A.D. Rao, A thermodynamic analysis of tubular SOFC based hybrid systems, Ph.D. Thesis, University of California, Irvine, USA, 2001.
[13] A. Verma, A.D. Rao, G.S. Samuelsen, J. Power Sources 158 (2006) 417–427.
[14] D.J. Palmer, A combined gas cooled nuclear reactor and fuel cell cycle, Ph.D. Thesis, Polytechnic University, New York, USA, 2006.
[15] K. Rajashekara, IEEE Trans. Ind. Appl. 41 (2005) 682–689.
[16] J. Lawrence, M. Boltze, J. Power Sources 154 (2006) 479–488.
[17] J.L. Martin, Fuel Cell Seminar: Fuel Cells in Paradise—30th Anniversary, Hawaii, November 13–17, 2006.
[18] A.L. Dicks, R.G. Fellows, C. Martin Mescal, C. Seymour, J. Power Sources 86 (2000) 501–506.
[19] F. Zink, Y. Lu, L. Schaefer, Energy Convers. Manage. 48 (2007) 809–818.
[20] S. McIntosh, R.J. Gorte, Chem. Rev. 104 (2004) 4845–4865.
[21] S. Park, R. Craciun, J.M. Vohs, R.J. Gorte, J. Electrochem. Soc. 146 (1999) 3603–3605.
[22] M. Mogensen, K. Kammer, Annu. Rev. Mater. Res. 33 (2003) 321–331.
[23] R.A. Roberts, J. Brouwer, ASME J. Fuel Cell Sci. Technol. 3 (2006) 18–25.
[24] M.G. Pangalis, R.F. Martinez-Botas, N.P. Brandon, Proc. Inst. Mech. Eng. A: J. Power Energy 216 (2002) 129–144.
[25] R.A. Georgr, J. Power Sources 86 (2000) 134–139.
[26] S.E. Veyo, L.A. Shockling, J.T. Dederer, J.E. Gillett, W.L. Lundberg, ASME J. Eng. Gas Turbines Power 124 (2002) 845–849.
[27] S.H. Chan, H.K. Ho, Y. Tian, J. Power Sources 114 (2003) 213–227.
[28] S.H. Chan, H.K. Ho, Y. Tian, J. Power Sources 109 (2002) 111–120.
[29] S.H. Chan, C.F. Low, O.L. Ding, J. Power Sources 203 (2002) 188–2000.
[30] S.H. Chan, H.K. Ho, Y. Tian, Int. J. Hydrogen Energy 28 (2003) 889–900.
[31] S. Campanari, ASME J. Eng. Gas Turbines Power 122 (2000) 239–246.
[32] D. Tucker, L. Lawson, R.S. Gemmen, R. Dennis, Evaluation of hybrid fuel cell turbine system startup with compressor bleed, ASME Paper GT2005-68784, 2005.
[33] D. Tucker, L. Lawson, J. VanOsdol, J. Kislear, A. Akinbobuyi, Examination of ambient pressure effects on hybrid solid oxide fuel cell turbine system operation using hardware simulation, ASME Paper GT2006-91291, 2006.
[34] E. Liese, R.S. Gemmen, Performance comparison of internal reforming against external reforming in a SOFC, Gas turbine hybrid system, ASME Paper, GT2003-38566, 2003.
[35] R.S. Gemmen, E. Liese, J.G. Rivera, F. Jabbari, J. Brouwer, Proceedings of ASME Turbo Expo 2000, 2000 (2000-GT-554).
[36] X. Zhang, J. Li, G. Li, Z. Feng, J. Power Sources 123 (2006) 523–531.
[37] A.F. Massardo, C.F. McDonald, T. Korakianitis, ASME J. Eng. Gas Turbines Power 124 (2002) 110–116.
[38] R.A. Roberts, J. Brouwer, G.S. Samuelsen, Fuel cell/gas turbine hybrid system control for daily load profile and ambient condition variation, ASME Paper GT2006-90741, 2006.
[39] T. Kaneko, J. Brouwer, G.S. Samuelsen, J. Power Sources 160 (2006) 316–325.
[40] A. Traverso, A. Massardo, R.A. Roberts, J. Brouwer, S. Samuelsen, ASME J. Fuel Cell Sci. Technol. 4 (2007) 373–383.
[41] P. Costamagna, L. Magistri, A.F. Massardo, J. Power Sources 96 (2001) 352–368.
[42] J. Palsson, A. Selimovil, L. Sjunnesson, J. Power Sources 86 (2000) 442–448.
[43] F. Calise, A. Palombo, L. Vanoli, J. Power Sources 158 (2006) 225–244.
[44] W.J. Yang, S.K. Park, T.S. Kim, J.H. Kim, J.L. Sohn, S.T. Ro, J. Power Sources 160 (2006) 462–473.
[45] S. Kimijima, N. Kasagi, Proceedings of ASME Turbo Expo 2002, Amsterdam, The Netherlands, 2002.
[46] W.L. Lundberg, S.E. Veyo, M.D. Moeckel, ASME J. Eng. Gas Turbines Power 125 (2003) 51–58.
[47] T. Kabata, M. Nishiura, K. Tomida, S. Koga, N. Matake, et al., 2008 Fuel Cell Seminar & Exposition, Phoenix, 2008, pp. 263–267 (DEM41-2).
[48] G.J. Williams, A. Siddle, K. Pointon, Design optimization of a hybrid solid oxide fuel cell & gas turbine power generation system, ALSTOM Power Technology Centre Report, 2001.
[49] Y. Yi, A.D. Rao, J. Brouwer, G. Scott Samuelsen, J. Power Sources 132 (2004) 77–85.
[50] C. Cunnel, M.G. Pangalis, R.F. Martinez-Botas, Proc. Inst. Mech. Eng. A: J. Power Energy 216 (2002) 145–154.
[51] X. Zhang, J. Li, G. Li, Z. Feng, J. Power Sources 164 (2007) 752–760.
[52] T. Araki, T. Ohba, S. Takezawa, K. Onda, Y. Sakaki, J. Power Sources 158 (2006) 52–59.
[53] T. Araki, T. Taniuchi, D. Sunakawa, M. Nagahama, K. Onda, T. Kato, J. Power Sources 171 (2007) 464–470.
[54] K. Onda, T. Iwanari, N. Miyauchi, K. Ito, T. Ohba, Y. Sakaki, S. Nagata, J. Electrochem. Soc. 150 (12) (2003) A1569–A1576.
[55] H. Lee Willis, W.G. Scott, Distributed Power Generation: Planning and Evaluation, CRC Press, 2000.
[56] H.E. Vollmar, C.U. Maier, C. Nolscher, T. Merklein, M. Poppinger, J. Power Sources 86 (2000) 90–97.
[57] K. Subramanyan, U.M. Diwekar, A. Goyal, J. Power Sources 132 (2004) 99–112.
[58] M. Yokoo, T. Take, J. Power Sources 137 (2004) 206–215.
[59] M. Yokoo, K. Watanabe, M. Arakawa, Y. Yamazaki, J. Power Sources 153 (2006) 18–28.
[60] N. Sakai, K. Yamaji, H. Negishi, T. Horita, Y.P. Xiong, H. Yokokawa, The Electrochemical Society Proceedings, vol. PV2001-16, 2001, pp. 511–520.
[61] M. Yokoo, K. Watanabe, M. Arakawa, Y. Yamazaki, J. Power Sources 159 (2006) 836–845.
[62] W. Winkler, H. Lorenz, J. Power Sources 105 (2002) 222–227.
[63] P. Kuchonthara, S. Bhattacharya, A. Tsutsumi, J. Power Sources 124 (2003) 65–75.
[64] F. Calise, M. Dentice, d'Accadia, A. Palombo, L. Vanoli, Energy 31 (2006) 3278–3299.
[65] M. Cali, M.G.L. Santarelli, P. Leone, J. Power Sources 156 (2006) 400–423.
[66] R.A. George, J. Power Sources 86 (2000) 134–139.
[67] Siemens celebrates one-year anniversary of SOFC generator in Italy, Fuel Cells Bull. September (2006) 3.
[68] M. Suzuki, T. Sogi, K. Higaki, T. Ono, N. Takahashi, K. Shimazu, T. Shigehisa, ECS Trans. 7 (2007) 27–30.
[69] E. Fontell, T. Kivisaari, N. Christiansen, J.-B. Hansen, J. Pålsson, J. Power Sources 131 (2004) 49–56.
[70] R.J. Braun, S.A. Klein, D.T. Reindl, Assessment of solid oxide fuel cells in building applications, Report Summary of Solar Energy Laboratory, University of Wisconsin-Madison, 2001.
[71] A.D. Hawkes, P. Aguiar, C.A. Hernandez-Aramburo, M.A. Leach, N.P. Brandon, et al., J. Power Sources 156 (2006) 321–333.
[72] E. Riensche, U. Stimming, G. Unverzagt, J. Power Sources 73 (1998) 251–256.
[73] E. Riensche, J. Meosinger, U. Stimming, G. Unverzagt, J. Power Sources 71 (1998) 306–314.
[74] J. Luz Silveira, E.M. Leal, L.F. Ragonha Jr., Energy 26 (2001) 891–904.
[75] A.W. Bett, O.V. Sulima, Semicond. Sci. Technol. 18 (2003) S184–S190.
[76] B. Bitnar, Semicond. Sci. Technol. 18 (2003) S221–S227.
[77] T.J. Coutts, J.P. Benner, C.S. Allman, Thermophotovoltaic Generation of Electricity: Fourth NREL Conference, Denver, CO, October, 1998 (AIP: NY).
[78] S. Basu, Y.B. Chen, Z.M. Zhang, Int. J. Energy Res. 31 (2007) 689–716.
[79] T.J. Coutts, Solar Energy Mater. Solar Cells 66 (2001) 443–452.
[80] D. Wilt, D. Chubb, D. Wolford, P. Magari, C. Crowley, CP890, Thermophotovoltaic Generation of Electricity, The Seventh Conference, 2007 (AIP 978-0-7354-0392-5).
[81] G.W. Charache, P.F. Baldasaro, L.R. Danielson, D.M. DePoy, et al., J. Appl. Phys. 85 (1999) 2247–2252.
[82] T.J. Coutts, G. Guazzoni, J. Luther, Thermophotovoltaic Generation of Electricity: Fifth Conference on Thermophotovoltaic Generation of Electricity, Rome, Italy, September, 2002.
[83] L.C. Brown, G.E. Besenbruch, R.D. Lentsch, K.R. Schultz, et al., High efficiency generation of hydrogen fuels using nuclear power, Final report to DOE, General Atomics report GA-A24285, June 2003.
[84] K.R. Schultz, World Nuclear Association Annual Symposium, London, September, 2003.
[85] D.J.L. Brett, P. Aguiar, N.P. Brandon, R.N. Bull, R.C. Galloway, et al., J. Power Sources 157 (2006) 782–798.
[86] S. Mukerjee, M.J. Grieve, K. Haltiner, M. Faville, J. Noetzel, et al., Proceedings of the SOFC VII, The Electrochemical Society, New Jersey, 2001 (PV 2001-16).
[87] C. Wang, Modeling and control of hybrid wind/photovoltaic/fuel cell distributed generation systems, Ph.D. Dissertation, Montana State University, Bozeman, Montana, 2006.
[88] P. Hollmuller, J.-M. Joubert, B. Lachal, K. Yvon, Int. J. Hydrogen Energy 25 (2000) 97–109.
[89] D.J. Bents, The 22nd Intersociety Energy Conversion Engineering Conference, Pennsylvania, August, 1987 (AIAA-87-9203).
[90] C. Severin, S. Pischinger, J. Ogrzewalla, J. Power Sources 145 (2005) 675–682.
[91] P. Lamp, J. Tachtler, O. Finkenwirth, S. Mukerjee, S. Shaffer, Fuel Cells 3 (2003) 143–152.
[92] A. Lindermeir, S. Kah, S. Kavurucu, M. Muhlner, Appl. Catal. B: Environ. 70 (2007) 488–497.
[93] Y. Yi, A.D. Rao, J. Brouwer, G. Scott Samuelsen, J. Power Sources 144 (2005) 67–76.
[94] S. Roychoudhury, M. Lyubovsky, D. Walsh, D. Chu, E. Kallio, J. Power Sources 160 (2006) 510–513.
[95] B. Braun, K. Fischer, M. Rzepka, U. Stimming, J.W. Biermann, M. Johannaber, H. Wallentowitz, Fuel Cells 3 (2003) 122–127.
[96] J.J. Krummenacher, K.N. West, L.D. Schmidt, J. Catal. 215 (2003) 332–343.
[97] B. Monnerat, L. Kiwi-Minsker, A. Renken, Chem. Eng. Sci. 56 (2001) 633–639.

[98] D. Shekhawat, D.A. Berry, T.H. Gardner, D.J. Haynes, J.J. Spivey, J. Power Sources 168 (2007) 477–483.
[99] Versa SOFC validated for hybrid automotive applications, Fuel Cells Bull. August (8) (2007).
[100] D.J.L. Brett, P. Aguiar, N.P. Brandon, J. Power Sources 163 (2006) 514–522.
[101] Th. Seitarides, C. Athanasiou, A. Zabaniotou, Renew. Sustain. Energy Rev. 12 (2008) 1251–1276.
[102] P. McKendry, Bioresour. Technol. 83 (2002) 55–63.
[103] C. Athanasiou, F. Coutelieris, E. Vakouftsi, V. Skoulou, et al., Int. J. Hydrogen Energy 32 (2007) 337–342.
[104] H. Hofbauer, R. Rauch, K. Bosch, R. Koch, C. Aichernig, in: A.V. Bridgewatter (Ed.), Pyrolysis and Gasification of Biomass and Waste, CPL Press, Newbury, UK, 2003.
[105] K.D. Panopoulos, L. Fryda, J. Karl, S. Poulou, E. Kakaras, J. Power Sources 159 (2006) 570–585.
[106] A.O. Omosun, A. Bauen, N.P. Brandon, C.S. Adjiman, D. Hart, J. Power Sources 131 (2004) 96–106.
[107] S. Cordiner, M. Feola, V. Mulone, F. Romanelli, Appl. Therm. Eng. 27 (2007) 738–747.
[108] J. Van herle, F. Marechal, S. Leuenderger, D. Favrat, J. Power Sources 118 (2005) 375–383.
[109] L. Fryda, K.D. Panopoulos, E. Kakaras, Energy Convers. Manage. 49 (2008) 281–290.
[110] M. Sucipta, S. Kimijima, K. Suzuki, J. Power Sources 174 (2007) 124–135.
[111] K. Agbossou, R. Chahine, J. Hamelin, F. Laurencelle, et al., J. Power Sources 96 (2001) 168–172.
[112] O. Ulleberg, S.O. Morner, Solar Energy 59 (1997) 271–279.
[113] Th.F. El-Shatter, M.N. Eskandar, M.T. El-Hagry, Renew. Energy 27 (2002) 479–485.
[114] J.D. Maclay, J. Brouwer, G.S. Samuelsen, Int. J. Hydrogen Energy 31 (2006) 994–1009.
[115] M. Little, M. Thomson, D. Infield, Int. J. Hydrogen Energy 32 (2007) 1582–1588.
[116] D. Shapiro, J. Duffy, M. Kimble, M. Pien, Solar Energy 79 (2005) 544–550.
[117] A. Demin, E. Gorbova, P. Tsiakaras, J. Power Sources 171 (2007) 205–211.
[118] M. Ni, M.K.H. Leung, D.Y.C. Leung, J. Power Sources 163 (2006) 460–466.
[119] M. Ni, M.K.H. Leung, D.Y.C. Leung, Int. J. Hydrogen Energy 32 (2007) 2305–2313.
[120] M. Mogensen, S. Primdahl, M. Jergensen, C. Bagger, J. Electroceram. 52 (2000) 141–152.
[121] J.S. Herringa, J.E. O'Brien, C.M. Stootsa, G.L. Hawkes, et al., Int. J. Hydrogen Energy 32 (2007) 440–450.
[122] O.A. Marina, L.R. Pederson, M.C. Williams, G.W. Coffey, et al., J. Electrochem. Soc. 154 (2007) B452–B459.
[123] J.E. O'Brien, C.M. Stoots, J.S. Herring, P.A. Lessing, ASME J. Fuel Cell Sci. Technol. 2 (2005) 156–163.
[124] S.H. Jensen, Solid oxide electrolyser cell, Ph.D. Thesis, Risø National Laboratory, Denmark, 2006.
[125] B. Wong, R.T. Buckinghama, L.C. Brown, B.E. Russ, G.E. Besenbruch, et al., Int. J. Hydrogen Energy 32 (2007) 497–504.
[126] L.M. Crosbie, D. Chapin, Hydrogen production by nuclear heat, GENES4/ANP2003, Paper 022703, Kyoto, Japan, 15–19 September 2003.
[127] P.M. Mathias, L.C. Brown, The 68th Annual Meeting of the Society of Chemical Engineers, Japan, March, 2003.
[128] Y. Kondou, S. Someya, IEEE Trans. 1 (2007) 22–26.
[129] A.C. Marshall, An assessment of reactor types for thermochemical hydrogen production. Final Report to DOE: SAND2002-0513, Sandia National Laboratories, Albuquerque, USA, 2002.
[130] A.D. Rao, G.S. Samuelsen, F.L. Robson, B. Washom, S.G. Berenyi, Advanced power plant development and analyses methodologies. Final Report to DOE of U.S., DE-FC26-00NT40845, October 2006.
[131] S. Ghosha, S. De, Energy 31 (2006) 345–363.
[132] J. Ratafia-Brown, L. Manfredo, J. Hoffmann, M. Ramezan, Major environmental aspects of gasification-based power generation technologies. Final Report to DOE of U.S., National Energy Technology Laboratory, WV, 2002.
[133] B.F. Möller, J. Arriagada, M. Assadi, I. Potts, J. Power Sources 131 (2004) 320–326.
[134] A.D. Rao, G.S. Samuelsen, ASME J. Eng. Gas Turbines Power 125 (2003) 59–66.
[135] SECA wraps first phase with SOFCs on way to commercial reality, Fuel Cells Bull. 7 (2007) 7.
[136] M.C. Williams, J.P. Strakey, S.C. Singhal, J. Power Sources 131 (2004) 79–85.
[137] Residential SOFCs making a big splash in Europe, Fuel Cells Bull. 8 (2007) 1.
[138] F. Jurado, J.R. Saenz, IEEE Trans. Energy Convers. 18 (2003) 342–347.
[139] X. Zhang, J. Li, G. Li, Z. Feng, J. Power Sources 160 (2006) 258–267.
[140] X. Zhang, S.H. Chan, H.K. Ho, J. Li, G. Li, Z. Feng, Int. J. Hydrogen Energy 33 (2008) 2355–2366.
[141] Y. Zhu, K. Tomsovic, Electric Power Syst. Res. 62 (2002) 1–11.
[142] R. Roberts, J. Brouwer, E. Liese, R.S. Gemmen, Development of controls for dynamic operation of carbonate fuel cell–gas turbine hybrid systems, ASME Paper GT2005-68774, 2005.
[143] R. Roberts, J. Brouwer, F. Jabbari, T. Junker, H. Ghezel-Ayagh, J. Power Sources 161 (2006) 484–491.
[144] F. Mueller, J. Brouwer, F. Jabbari, S. Samuelsen, ASME J. Fuel Cell Sci. Technol. 3 (2006) 144–154.
[145] F. Mueller, F. Jabbari, J. Brouwer, R. Roberts, et al., ASME J. Fuel Cell Sci. Technol. 4 (2007) 221–230.
[146] C. Stiller, B. Thorud, O. Bolland, R. Kandepu, L. Imsland, J. Power Sources 158 (2006) 303–315.
[147] A.K.M. M. Murshed, B. Huang, K. Nandakumar, J. Power Sources 163 (2007) 830–845.
[148] M.R. Haines, W.K. Heidug, K.J. Li, J.B. Moore, J. Power Sources 106 (2002) 377–380.
[149] B.F. Moller, J. Arriagada, M. Assadi, I. Potts, J. Power Sources 131 (2004) 320–326.
[150] J.W. Dijkstra, D. Jansen, Energy 29 (2004) 1249–1257.
[151] R. Bredesen, K. Jordal, O. Bolland, Chem. Eng. Process. 43 (2004) 1129–1158.